



# Holographic Interferometry and Image Analysis for Aerodynamic Testing

J. E. O'Hare and W. T. Strike  
ARO, Inc.

September 1980

Final Report for Period October 1, 1976 — September 30, 1978

Approved for public release; distribution unlimited.

Property of U. S. Air Force  
AEDC LIBRARY  
F1980-77-C-0003

**ARNOLD ENGINEERING DEVELOPMENT CENTER  
ARNOLD AIR FORCE STATION, TENNESSEE  
AIR FORCE SYSTEMS COMMAND  
UNITED STATES AIR FORCE**

## NOTICES

When U. S. Government drawings, specifications, or other data are used for any purpose other than a definitely related Government procurement operation, the Government thereby incurs no responsibility nor any obligation whatsoever, and the fact that the Government may have formulated, furnished, or in any way supplied the said drawings, specifications, or other data, is not to be regarded by implication or otherwise, or in any manner licensing the holder or any other person or corporation, or conveying any rights or permission to manufacture, use, or sell any patented invention that may in any way be related thereto.

Qualified users may obtain copies of this report from the Defense Technical Information Center.

References to named commercial products in this report are not to be considered in any sense as an indorsement of the product by the United States Air Force or the Government.

This report has been reviewed by the Office of Public Affairs (PA) and is releasable to the National Technical Information Service (NTIS). At NTIS, it will be available to the general public, including foreign nations.

## APPROVAL STATEMENT

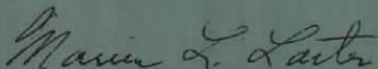
This report has been reviewed and approved.



MARSHALL K. KINGERY  
Project Manager  
Directorate of Technology

Approved for publication:

FOR THE COMMANDER



MARION L. LASTER  
Director of Technology  
Deputy for Operations

# UNCLASSIFIED

REPORT DOCUMENTATION PAGE		READ INSTRUCTIONS BEFORE COMPLETING FORM
1 REPORT NUMBER AEDC-TR-79-75	2 GOVT ACCESSION NO.	3 RECIPIENT'S CATALOG NUMBER
4 TITLE (and Subtitle) HOLOGRAPHIC INTERFEROMETRY AND IMAGE ANALYSIS FOR AERODYNAMIC TESTING	5 TYPE OF REPORT & PERIOD COVERED Final Report, Oct 1, 1976 - Sept 30, 1978	
	6 PERFORMING ORG REPORT NUMBER	
7 AUTHOR(s) J. E. O'Hare and W. T. Strike, ARO, Inc., a Sverdrup Corporation Company	8 CONTRACT OR GRANT NUMBER(s)	
9 PERFORMING ORGANIZATION NAME AND ADDRESS Arnold Engineering Development Center/DOT Air Force Systems Command Arnold Air Force Station, Tennessee 37389	10 PROGRAM ELEMENT, PROJECT, TASK AREA & WORK UNIT NUMBERS Program Element 65807F	
11 CONTROLLING OFFICE NAME AND ADDRESS Arnold Engineering Development Center/DOS Air Force Systems Command Arnold Air Force Station, Tennessee 37389	12 REPORT DATE September 1980	
	13 NUMBER OF PAGES 42	
14 MONITORING AGENCY NAME & ADDRESS (if different from Controlling Office)	15 SECURITY CLASS (of this report)  UNCLASSIFIED	
	15a DECLASSIFICATION/DOWNGRADING SCHEDULE N/A	
16 DISTRIBUTION STATEMENT (of this Report)  Approved for public release; distribution unlimited.		
17 DISTRIBUTION STATEMENT (of the abstract entered in Block 20, if different from Report)		
18 SUPPLEMENTARY NOTES  Available in Defense Technical Information Center (DTIC)		
19 KEY WORDS (Continue on reverse side if necessary and identify by block number) holography                      flow fields interferometry                data acquisition images                            supersonic flow aerodynamics                hypersonic flow wind tunnels		
20 ABSTRACT (Continue on reverse side if necessary and identify by block number) This report summarizes the progress achieved in the von Kármán Gas Dynamics Facility (VKF) of the Arnold Engineering Development Center (AEDC), Air Force Systems Command (AFSC) in the: (1) development of operational techniques and hardware for recording holographic interferograms in the VKF wind tunnels, (2) development of automated image analysis techniques for reducing quantitative flow-field data from holographic		

# UNCLASSIFIED

# UNCLASSIFIED

## 20. ABSTRACT (Continued)

interferograms, and (3) investigation and development of software for the application of digital image analysis to other photographic techniques used in wind tunnel testing.

## PREFACE

The work reported herein was conducted by the Arnold Engineering Development Center (AEDC), Air Force Systems Command (AFSC), and Marshall K. Kingery, AEDC/DOTR, was the Air Force project manager. The results were obtained by ARO, Inc., AEDC Division (a Sverdrup Corporation Company), operating contractor for the AEDC, AFSC, Arnold Air Force Station, Tennessee. The work was conducted under ARO Project No. V32I-P3A.

Many people at AEDC contributed to this project and are acknowledged for their work. Special recognition is given to ARO, Inc. employees, Mr. W. L. Templeton for the experimental work with the holographic flow visualization systems, Mr. T. E. Gwynn, Jr. for the software development for image analysis, and Mr. L. L. Leach for the development of the software for the numerical data reduction.

## CONTENTS

	<u>Page</u>
1.0 INTRODUCTION .....	5
2.0 HOLOGRAPHIC FLOW VISUALIZATION SYSTEMS	
2.1 Transmission Holographic Flow Visualization System .....	7
2.2 Diffuse Reflection Holographic Flow Visualization System .....	10
2.3 Holographic Quality Pulsed Ruby Laser .....	11
3.0 HOLOGRAPHIC RECONSTRUCTION SYSTEM .....	18
4.0 TRANSMISSION HOLOGRAPHIC FLOW VISUALIZATION	
4.1 Transmission Interferometry .....	21
4.2 Shadowgraph and Schlieren Reconstruction .....	23
5.0 DIFFUSE REFLECTION HOLOGRAPHIC FLOW VISUALIZATION	
5.1 Diffuse Reflection Interferometry .....	24
6.0 AUTOMATED INTERFEROGRAM ANALYSIS AND DATA REDUCTION	
6.1 Image Analyzer-Digitizer System .....	27
6.2 Interferometric Reconstruction and Digitization .....	28
6.3 Interferometric Fringe Measurements .....	29
6.4 Interferometric Data Reduction .....	30
7.0 IMAGE ANALYSIS APPLICATION TO OTHER AERODYNAMIC TESTING TECHNIQUES	
7.1 Geometric and Photometric Measurements .....	37
7.2 Photometric Corrections .....	37
7.3 Camera Perspective Modification .....	37
7.4 Photometric Data Presentation .....	39
8.0 CONCLUSIONS .....	39
REFERENCES .....	42

## ILLUSTRATIONS

### Figure

1. Flow-Field Hologram, 1968 Vintage .....	6
2. Transmitted Light Flow Visualization System .....	8
3. Glass Film Plate Holder .....	9

<u>Figure</u>	<u>Page</u>
4. Light Source, Transmission Holographic Flow Visualization System . . . . .	9
5. Portable Transmission Holographic Flow Visualization System . . . . .	10
6. Schematic of Diffuse Reflection Holographic Flow Visualization System . . . . .	11
7. Diffuse Reflection Holographic Flow Visualization System (RELI) . . . . .	12
8. Lab Setup - Diffuse Reflection Holographic Flow Visualization System . . . . .	14
9. Multimode Contour Lines . . . . .	15
10a. Interferogram Made with Multimode Laser Pulse . . . . .	16
10b. Interferogram Made with Single-Mode Laser Pulse . . . . .	16
11. Suppression of Longitudinal Multimodes by the Two Etalon System . . . . .	17
12. Control System Console . . . . .	19
13. Holographic Reconstruction System . . . . .	20
14. Diffuse Reflection Interferogram Reconstruction . . . . .	21
15. Interferogram Reconstruction, Transmitted Light . . . . .	22
16a. Shadowgraph Reconstruction . . . . .	23
16b. Schlieren Reconstruction . . . . .	24
17. Diffused Reflected Light Interferogram, Double Plate . . . . .	26
18. Diffused Reflected Light Interferogram, Time Difference . . . . .	27
19. Image Analyzer-Digitizer System . . . . .	28
20. Schematic of Image Analyzer-Digitizer System . . . . .	29
21. Digitized Image of Interferogram . . . . .	31
22. Fringe Centerline Tracking . . . . .	32
23. Digitized Fringe Shift Distribution . . . . .	33
24. Corrected Fringe Shift Distribution . . . . .	33
25. Normalized Fringe Shift Pattern . . . . .	34
26. Correlation of Fringe Shift Pattern . . . . .	35
27. Curve Fit of the Fringe Shift Data Distribution . . . . .	35
28. Density Distribution in the Flow Field of a Sphere . . . . .	36
29. Oblique Camera Perspective Correction . . . . .	38
30. Equal Density Contouring . . . . .	40
31. Digital Data - Pixel Grey Level Array of a Vortex . . . . .	41

## 1.0 INTRODUCTION

Since the first flow visualization hologram (Fig. 1) was recorded at the Arnold Engineering Development Center (AEDC), von Kármán Gas Dynamics Facility (VKF), Supersonic Wind Tunnel (D) in August 1968, significant progress has been made in the development of holographic flow visualization recording techniques. The replacement of temporary optical bench hardware, unreliable lasers, and manual data reduction methods with operational hardware and automated data reduction methods has been a gradual process. The purpose of this report is to present recent advances in the application of operational holographic systems, digital image analysis, and data reduction to aerodynamic testing in the VKF Supersonic and Hypersonic Wind Tunnels. Technology developed at AEDC and other facilities was utilized to develop and design operational holographic recording systems that would be reliable under the adverse environments characteristic of large supersonic and hypersonic wind tunnels. Digital image analysis and computer technology were used to develop data reduction methods to take advantage of the operational holographic recording capability. The primary objectives of this project were (1) to develop operational techniques and hardware for recording holographic interferograms in large wind tunnels, (2) to develop automated image analysis techniques for reducing quantitative flow-field data from holographic interferograms, and (3) to investigate the feasibility of and develop software for the application of digital image analysis to other photographic techniques used in wind tunnel testing.

This document describes the accomplishments achieved in meeting these objectives and presents examples of aerodynamic data recording in the VKF wind tunnels. Holographic techniques for aerodynamic testing have been extensively reported (see Refs. 1 through 7). The information contained in these references was utilized to aid in the development of the hardware and techniques described in this report.

Basic to all holographic flow visualization techniques is the concept that a coherent electromagnetic wave which has passed through a flow field is modulated in a manner which characterizes the flow field. The modulated wave can be recorded as a hologram by mixing it with an unmodulated coherent light wave. Essentially all types of optical flow visualization are combined into a single holographic recording in such a way that any specific technique can be applied. This method provides a means to freeze the flow-field information in time for retrieval at a later time under ideal laboratory conditions for as long as required to extract the desired information. Any visual or optical imaging technique such as shadowgraph, schlieren, or interferometry can be applied. Conventional interferometers are not practical to use around large wind tunnels because of the vibrational environment. Consequently, the holographic interferometry technique is of primary interest since quantitative information about the flow field can be obtained.

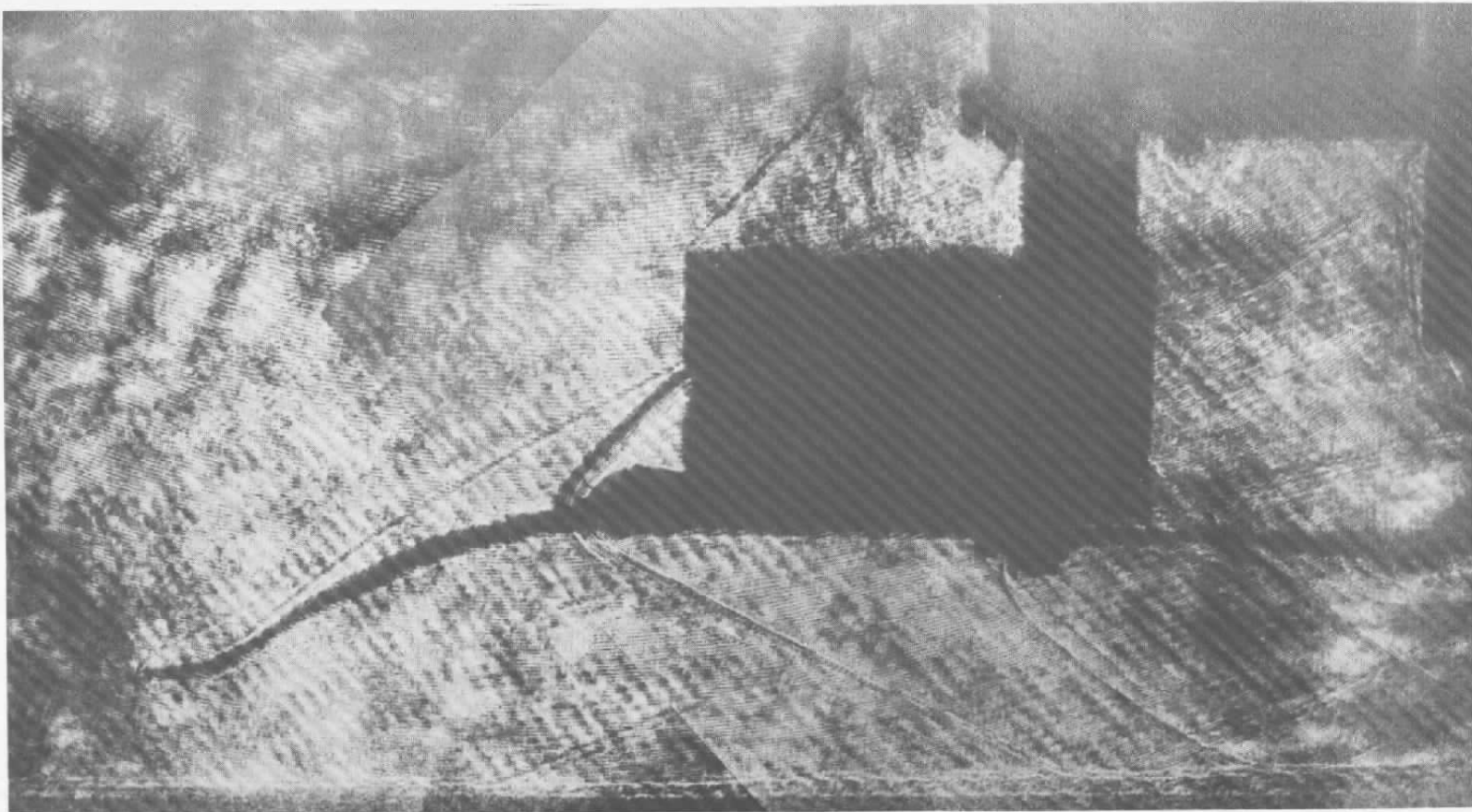


Figure 1. Flow-field hologram, 1968 vintage.

## 2.0 HOLOGRAPHIC FLOW VISUALIZATION SYSTEMS

Throughout the period of holographic technology development and experimentation in the VKF wind tunnels, temporary optical bench arrangements were used for convenience in mounting and adjusting experimental components. This method was useful for experimental purposes but required an excessive amount of setup time and frequent realignment. These experimental setups, although useful at the time, were not practical for use as operational systems which should approach turnkey operation in the final system design. Two operational systems were designed, one for transmission holographic flow visualization, and the other for diffuse reflection holographic flow visualization. The design criteria required the hardware to be portable, compact, easy and fast to set up, and require little or no realignment or adjustments during a normal wind tunnel operating shift. A ribbed aluminum plate was chosen as the base for mounting the laser and other optical components. A laser mount was provided in each system for the pulsed ruby laser so that it could be easily installed in either system with a minimum of realignment. Adjustable components were kept to a minimum to reduce the possibilities of misalignment caused by vibration or human knob turning. A protective cover was also provided to prevent a person from inadvertently viewing the laser beam. Interlocks were placed on several components to prevent the operator from charging the laser during alignment and to protect some of the optical components. Interlocks were installed on the autocollimator mount used for alignment of the ruby laser and the storage position for the transverse mode aperture. These interlocks are also in series with interlocks on the system control console discussed in Section 2.3.3.

### 2.1 TRANSMISSION HOLOGRAPHIC FLOW VISUALIZATION SYSTEM

The transmission holographic flow visualization system is a laser light source unit that is used in conjunction with conventional single-pass Topley schlieren system optics using the optical arrangement described in Ref. 6. It was designed to be mounted directly onto the conventional schlieren light source units in the VKF Tunnels B, C, and F or it can be used with a pair of 20-in.-diam portable paraboloidal schlieren mirrors. The holographic system is shown schematically in Fig. 2 in a typical VKF supersonic tunnel installation. A front surface mirror, M3, used in the conventional schlieren light source is utilized in this case to direct the object beam toward the first primary schlieren mirror. The laser is mounted at a height that permits the reference beam to be reflected from a flat front surface mirror, M4, directly across the top of the wind tunnel. The reference beam is then reflected from another flat front surface mirror, M5, on the opposite side of the wind tunnel to direct the reference beam toward the glass film plate holder used for the holographic recording (Fig. 3). The object beam, after traversing through the wind tunnel test section, is gathered by the second paraboloidal schlieren mirror and directed toward the holographic plate to mix with the reference beam.

The pulsed ruby laser, LA1, is on a self-aligning mount and is secured to the ribbed aluminum baseplate (Fig. 4). A 3-mw helium-neon (He-Ne) laser, LA2, is mounted beside the ruby laser on the same optical axis by using two flat front surface mirrors, M1 and M2 (see Figs. 2 and 4). The pulsed ruby laser is used for making the holographic recordings, whereas the helium-neon laser is used for alignment purposes only. A quartz wedge beam splitter, BS, is mounted directly in front of the pulsed ruby laser providing an object beam and reference beam. The reference beam is transmitted through the beam splitter and the object beam is reflected down at a 90-deg angle. A mount is provided for an autocollimator for the purpose of aligning the pulsed ruby laser. Another mount is provided to store the autocollimator when not in use and includes interlocks to prevent laser charging while the autocollimator is in its alignment position. Two lenses, L1 and L2, are provided for expanding and collimating the reference beam. Two lenses, L3 and L4, are provided below the base plate mounted in a tube for expansion of the object beam. When this system is used with the portable schlieren mirrors, a mirror, M3, can also be attached to the bottom of the object beam tube for direction of the object beam toward the first portable schlieren mirror (Fig. 5). Because of a relatively long coherence length (several meters) of the pulse emitted by this pulsed ruby laser, the path lengths are matched to  $\leq \pm 30$  cm.

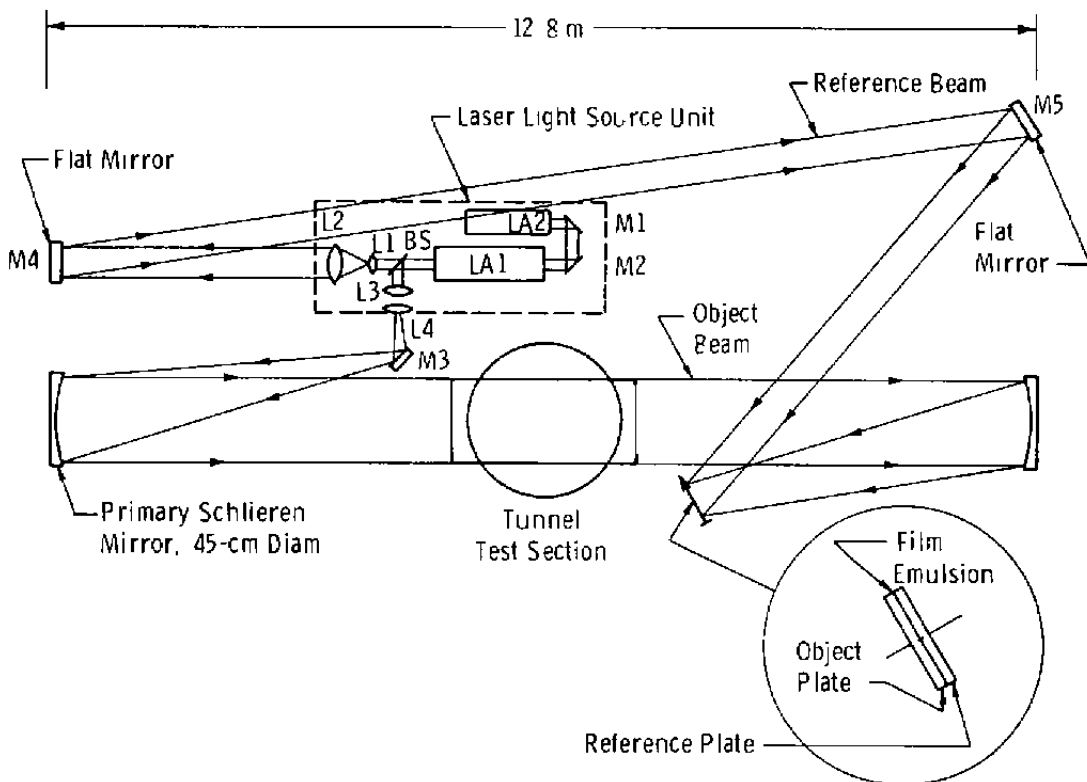


Figure 2. Transmitted light flow visualization system.

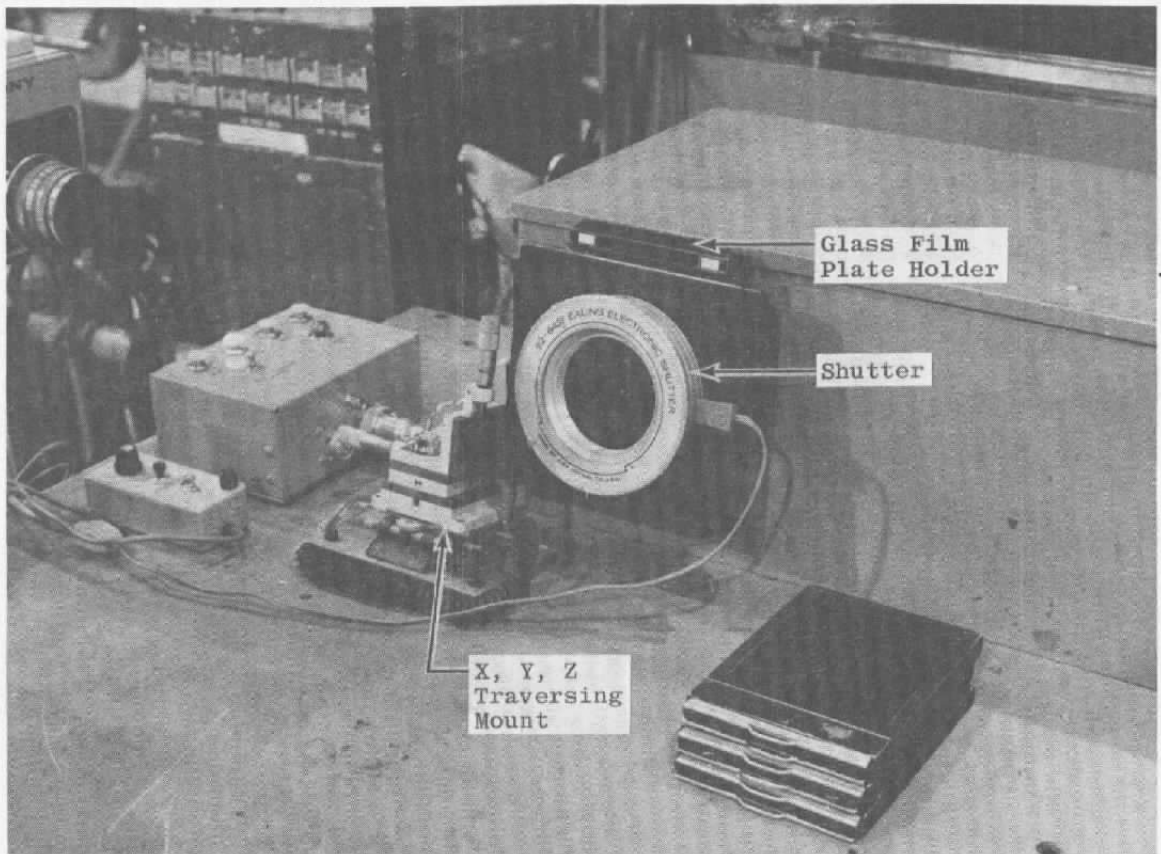


Figure 3. Glass film plate holder.

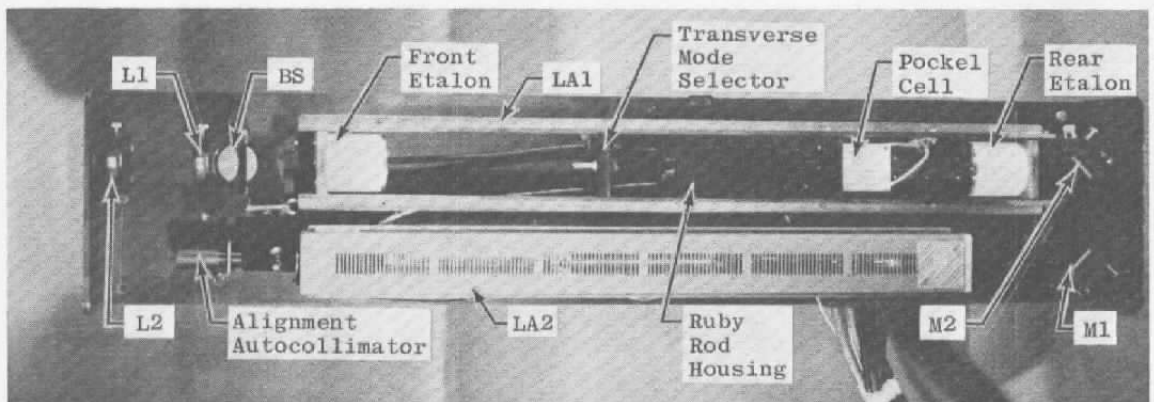


Figure 4. Light source, transmission holographic flow visualization system.

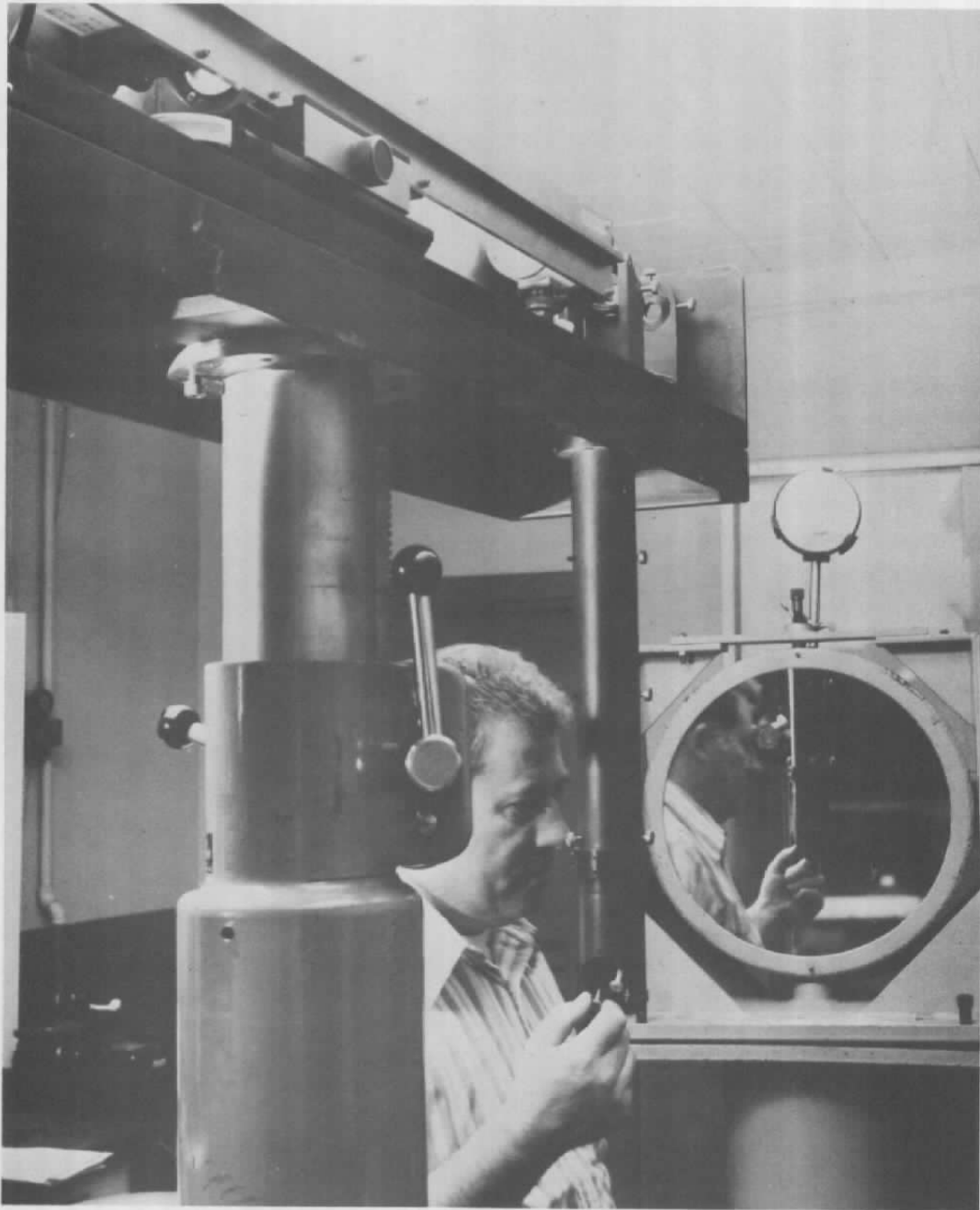
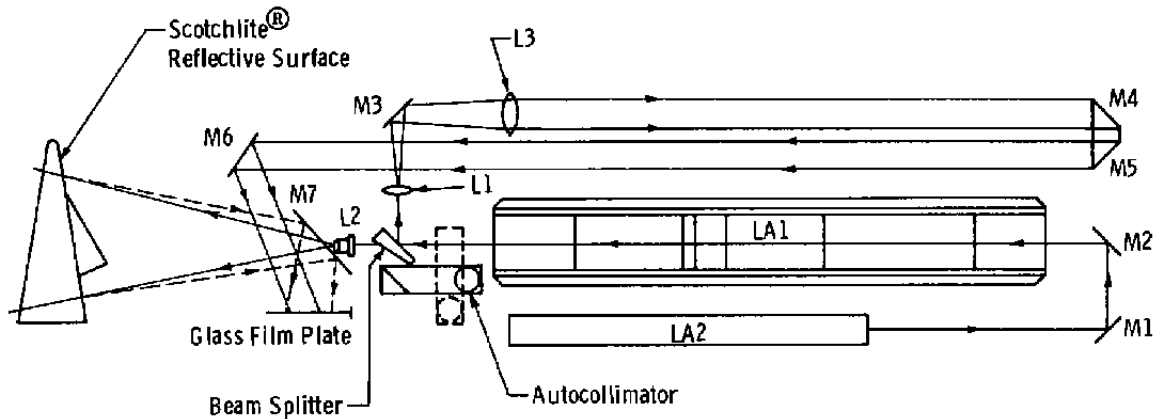


Figure 5. Portable transmission holographic flow visualization system.

## 2.2 DIFFUSE REFLECTION HOLOGRAPHIC FLOW VISUALIZATION SYSTEM

The diffuse reflection holographic flow visualization system (Fig. 6), unlike the transmission system previously described, is a stand-alone optical system that requires no



**Figure 6. Schematic of diffuse reflection holographic flow visualization system.**

external optical components to record diffused reflected light holograms or interferograms. The pulsed ruby laser, LA1, that is used for the holographic recordings is mounted on a self-aligning quick-mount and secured to a ribbed aluminum baseplate. A picture of this system is shown in Fig. 7. A 3-mw helium-neon laser, LA2, mounted adjacent to the pulsed laser is set up on the same optical axis as the pulsed laser by using two front surface mirrors, M1 and M2. The helium-neon laser is used for aligning the optical system and for directing the holographic system toward the object of interest. The beam splitter, BS, located directly in front of the ruby laser reflects the reference beam toward the beam expanding lens, L1, and transmits the object beam through lens L2 for expansion toward the object of interest. The reference beam, after expansion, is reflected from mirror M3 and collimated by lens L3. Mirrors M4 and M5 reflect the collimated reference beam toward mirror M6, which in turn reflects the reference beam onto the glass film plate. Mirrors M4 and M5 are mounted on a common mount which can be moved along the optical axis for optical path length matching of the object and reference beams. The adjustment provided in the length of the reference beam with mirrors M4 and M5 provides an optical system-to-object distance of from 68 to 106 cm. The object beam is expanded by lens L2 and proceeds through a hole in mirror M7 and impinges upon the reflective surface of interest. The light reflected from the diffuse reflective surface of interest is then reflected by mirror M7 onto the glass film plate where it is mixed with the reference beam. This system is shown in Fig. 8 in a laboratory setup with a typical wind tunnel model which was used in the experiments described in Section 5.1. A bright reconstruction of the reflective surface can be obtained with the surface painted white up to a diameter of 20 cm and up to a diameter of 90 cm with the surface painted with Scotchlite<sup>®</sup>.

### 2.3 HOLOGRAPHIC QUALITY PULSED RUBY LASER

It was recognized early in the development of holographic techniques for wind tunnel testing that one of the most important factors related to the quality of a holographic

reconstruction was the quality of the coherent light beam emitted by the pulsed ruby laser. It was also recognized that if holographic techniques were to be accepted as an operational diagnostic measurement method in large wind tunnels which produce large volumes of other types of data, the laser must be reliable and provide repeatable light source characteristics. At the beginning of this project in 1976 these requirements were beyond the state-of-the-art of pulsed ruby lasers. The lasers were not thermally stable and hence the cavity would not

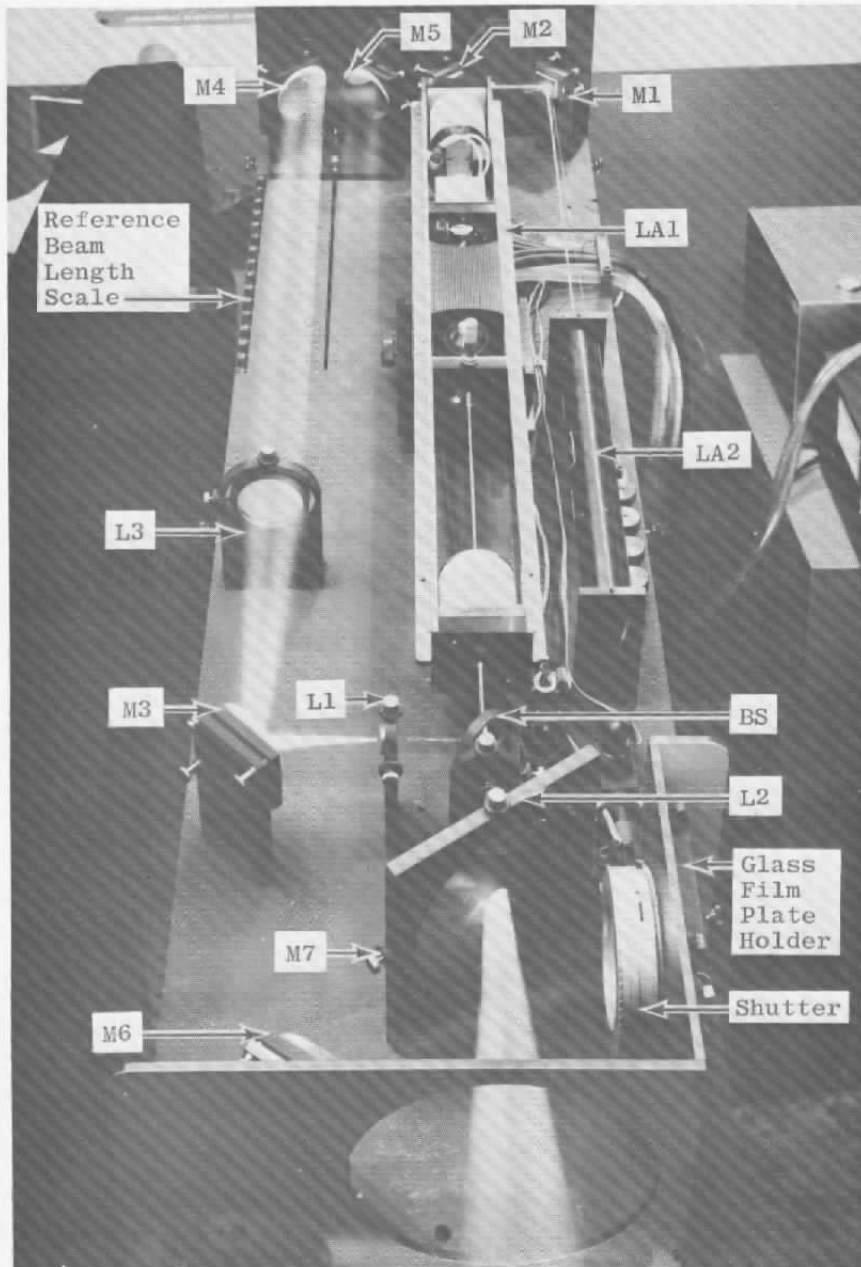


Figure 7. Diffuse reflection holographic flow visualization system (RELI).

stay in alignment. The quality (homogeneity) of the ruby rods was not satisfactory and the light beam was plagued with short coherence length and transverse and longitudinal multimodes. In retrospect, the poor quality of the first flow visualization hologram made in a VKF wind tunnel in August 1968 (Fig. 1) was attributed mainly to the poor quality of the light beam emitted by the pulsed ruby laser used for the recording.

Using technology available at the time and experimental knowledge of the problems associated with recording holograms with pulsed ruby lasers, specifications were written for a holographic quality pulsed ruby laser system. Particular emphasis was placed on beam quality, operational reliability, and alignment stability. These specifications could not be met with an off-the-shelf laser at that time. However, it was within the capabilities of the laser industry to produce a laser system which met the required specifications.

### **2.3.1 Operational Reliability**

The laser head component mount was specified to be stable for at least twenty-four hours at ambient temperatures from 70 to 90°F, and the components were to be mounted firmly to prevent misalignment caused by moderate vibration in a nonlaboratory environment. At the time of this procurement, all pulsed ruby lasers were laboratory models with adjustments on all components mounted on an optical bench. In general, these lasers required frequent adjustments in order to maintain satisfactory operation. These lasers were not reliable when subjected to the operational environment of a large wind tunnel. This operational problem was solved by mounting all the laser head components on Invar® side rails supported near their balance point (Fig. 8). Adjustments to the cavity were limited to the tilt of the front and rear etalons which were on stable kinematic mounts. The laser stayed in alignment over an ambient temperature range of 60 to 90°F in the wind tunnel environment over periods of several days.

### **2.3.2 Light Output Characteristics**

Specifications pertaining to the light output characteristics were all met by the manufacturer, Holobeam Laser, Inc., with the exception of line width (single line width of less than 0.01 Å). Transverse modes were adequately suppressed by a 2-mm-diam aperture in the laser cavity; however, under even the most favorable operating conditions, the laser beam emitted two spectral lines approximately 0.018-Å units apart. This longitudinal multimode output produced interferometric fringes in the laser beam caused by the interference of the two separate, closely spaced frequencies. When using the reflected light technique, this condition produced contour fringes on the surface of the wind tunnel model which represented equal distance contours of the model surface from a point on the laser



**Figure 8. Lab setup - diffuse reflection holographic flow visualization system.**

beam axis. Figure 9 is a reconstruction of a hologram of a typical wind tunnel model made with the reflection holographic system. These interference fringes were caused by the longitudinal multimode output of a single 17-msec pulse from the ruby laser. Since the desired data from a flow field are derived from interferometric fringes located in space in front of the model, these unwanted fringes on the model surface are detrimental to analyzing the data fringes. A concentrated effort, with the cooperation of the laser manufacturer, was directed to this problem since it directly affected the successful utilization of the diffuse reflected light holographic interferometry technique. Multimode pulses also reduce fringe contrast when using the transmission holographic technique. Figure 10a is a transmission holographic interferogram made with a multimode pulse from the pulsed ruby laser. Figure 10b is another transmission holographic interferogram made within a few minutes of the previous one with a single-mode pulse from the laser. The difference in fringe noise and contrast is obvious.

### 2.3.2.1 Laser Modification

Since a pulsed ruby laser is inherently a multimode device, steps must be taken to either filter or suppress unwanted modes (Fig. 11a). In the original configuration, the laser cavity utilized a temperature-tuned etalon as the front reflector and a mirror for the rear reflector. The front reflector was satisfactorily suppressing widely separated longitudinal modes but did not have a sufficiently narrow bandpass to adequately suppress modes that were closely spaced. The laser manufacturer developed a double temperature-tuned Fabry-Perot etalon system to replace the etalon-mirror system which served as the laser cavity reflectors. Tuning the etalons is accomplished by thermal expansion of the optically contacted spacers between the multiple etalon reflectors mounted on a thermally stable mount inside an oven. The newly developed front etalon, which serves as the front reflector, can be thermally tuned to suppress all but two or three of the very closely spaced spectral lines centered about the predominant line of the laser gain bandwidth (Fig. 11b). The rear etalon, which serves as the rear reflector, has a very narrow bandwidth of less than  $0.01 \text{ \AA}$  and can be thermally tuned to center on the predominant line and suppress the undesirable modes not suppressed by the front etalon (Fig. 11c). Laser cavity efficiency is reduced below lasing threshold at frequencies other than the etalon resonant frequencies resulting in a single-line output of less than  $0.01 \text{ \AA}$  (Fig. 11d).

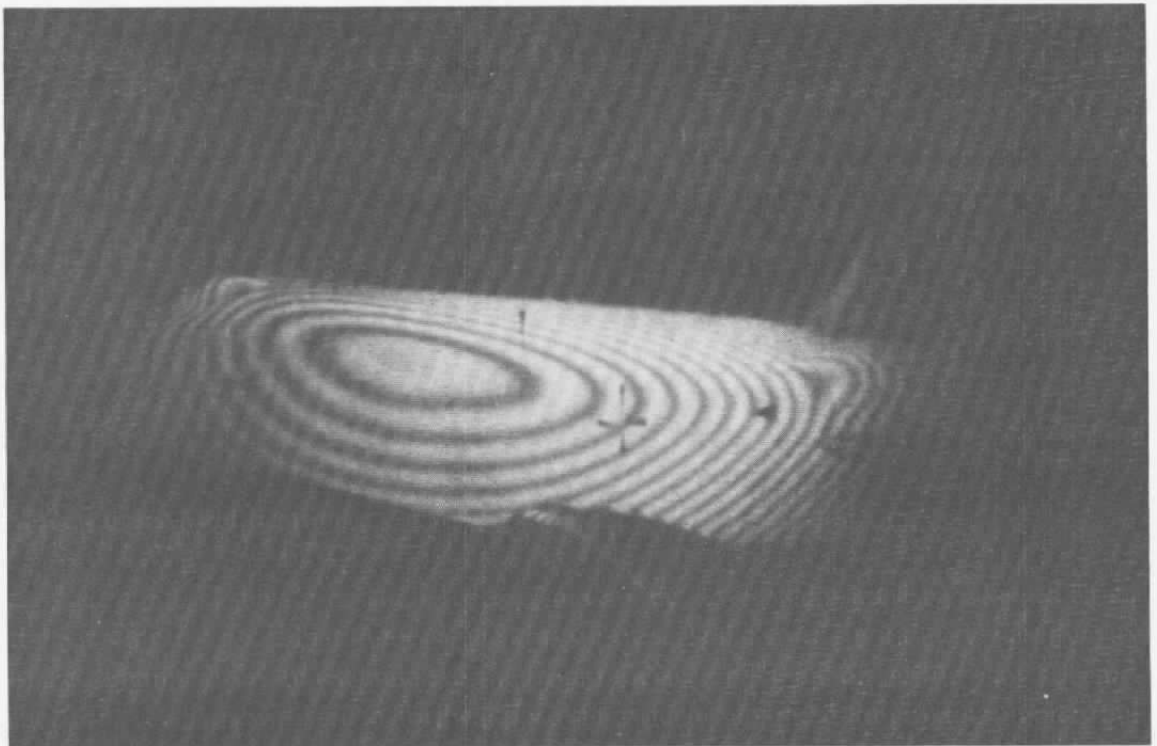


Figure 9. Multimode contour lines.

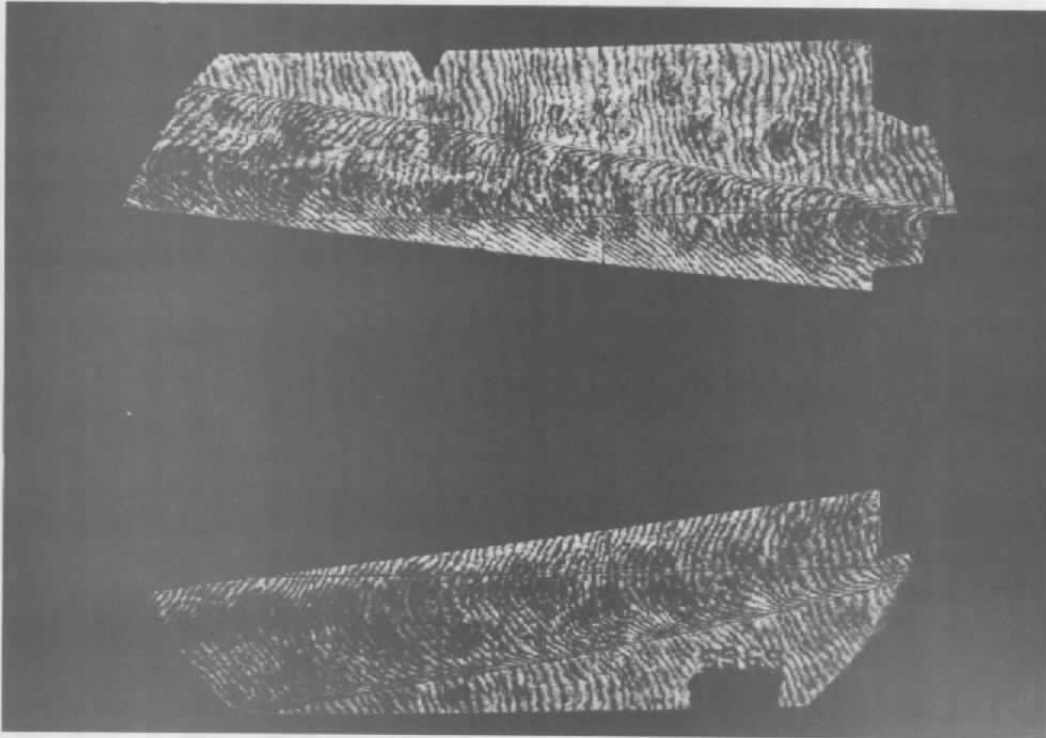


Figure 10a. Interferogram made with multimode laser pulse.

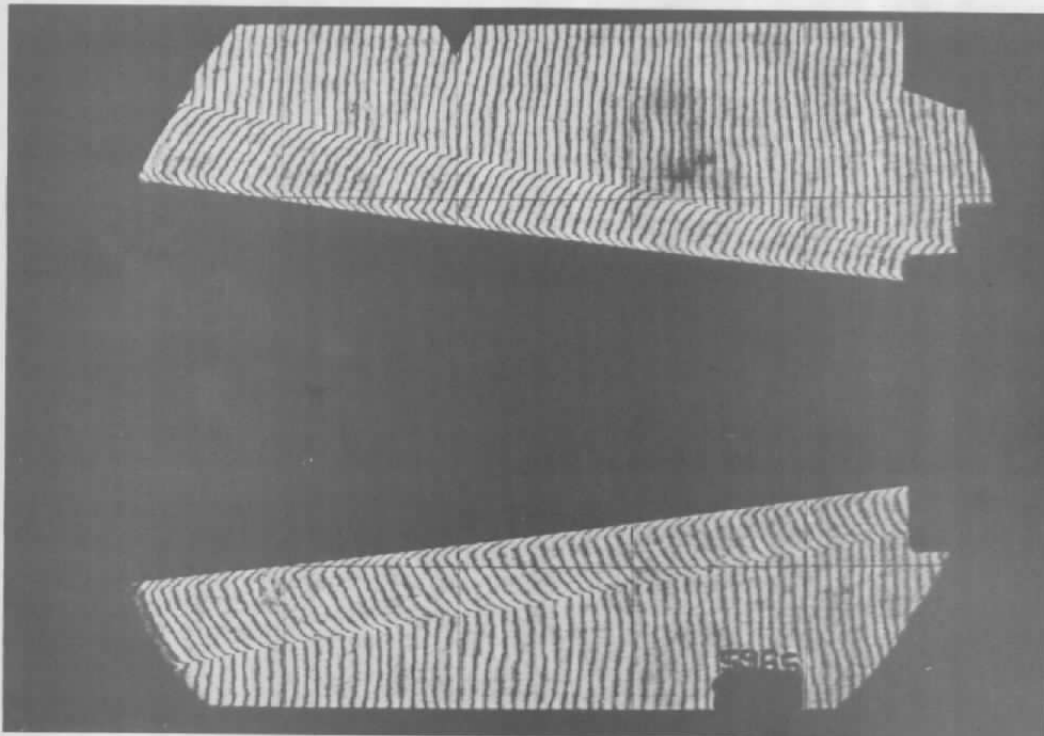
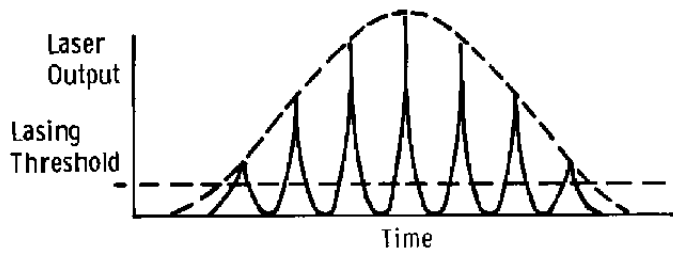
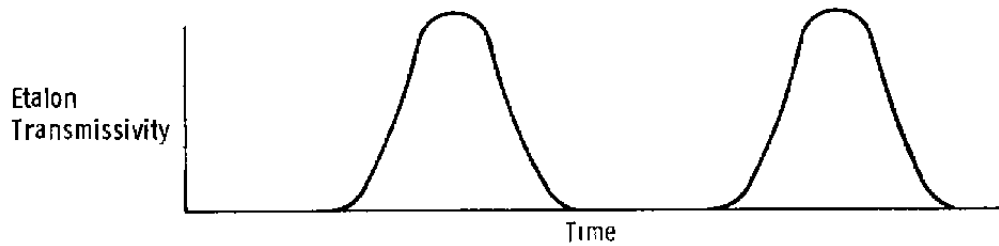


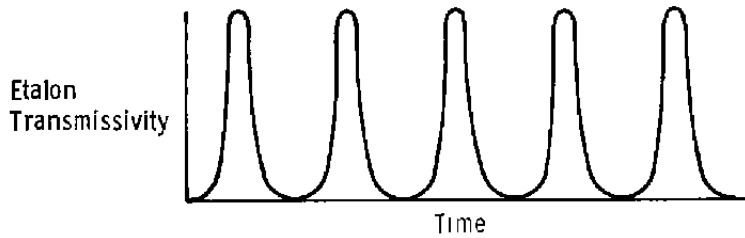
Figure 10b. Interferogram made with single-mode laser pulse.



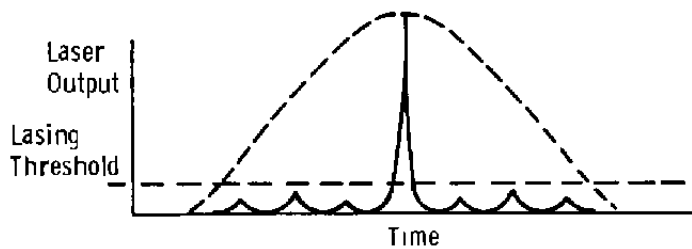
a. Representation of longitudinal multimode laser pulse



b. Front etalon bandpass



c. Rear etalon bandpass



d. Representation of single longitudinal mode laser pulse

Figure 11. Suppression of longitudinal multimodes by the two etalon system.

Optimum operating temperatures for properly tuning the etalons were determined by making a single-pulse hologram of a flat surface tilted 45 deg from the laser beam axis to provide a diffuse reflecting surface 1 m in depth along the optical axis. The maximum transmission or reflectance position of each etalon was shifted by changing its oven operating temperature in small increments and observing interference fringes, or, the absence thereof, on the image of the reflective surface reconstructed from the hologram. When no interference fringes were observed over the 1-m depth, the laser was emitting a single-mode coherent light pulse. The optimum operating temperatures for the etalons were the same after repeated laser cavity realignments and changes in ambient room temperature. These tests also verified the importance of a limitation in pumping the ruby rod to just above threshold to achieve consistent single-mode operation. This restraint prohibits increasing the laser output power by overpumping the laser cavity if single-mode light output is required. However, the output power obtained with the single-mode pulse is adequate for the applications described.

### 2.3.3 Laser Control System

A system was designed and installed in a console to control all the functions of the laser system and the holographic recording system (Fig. 12). Provisions were also made to interface this system with the wind tunnel data acquisition system to achieve remote and safe operation, and an indication of the time of holographic recordings. The system was built around the laser power supply, the power supply and controls for the Pockel cell Q-switch, and the water cooler used for cooling the flash lamp and ruby rod housing. Interlocks were also provided in series with safety interlocks in the laser head so the laser could not be inadvertently fired under conditions which would be dangerous to the operating personnel. Provision was made for monitoring the temperature of the cooling water and the temperature of the two temperature-tuned etalons at the control panel by observing a digital thermometer.

## 3.0 HOLOGRAPHIC RECONSTRUCTION SYSTEM

Components of the holographic reconstruction system are mounted on a 4- by 8-ft table which utilizes three pneumatic supports for table stability and vibration isolation (Fig. 13). A 50-mw continuous wave helium-neon laser is used to reconstruct the holograms. A double-glass plate holder described in Ref. 2 is used to hold either a single or a double holographic film plate. A collimator is provided on the helium-neon laser to duplicate the geometry of the reference beam used for recording the hologram. Two mirrors are utilized to provide the correct reference beam-to-holographic plate angle. The plate nearest the laser is initially aligned and held stationary, whereas the second plate is adjustable in X, Y, and



Figure 12. Control system console.

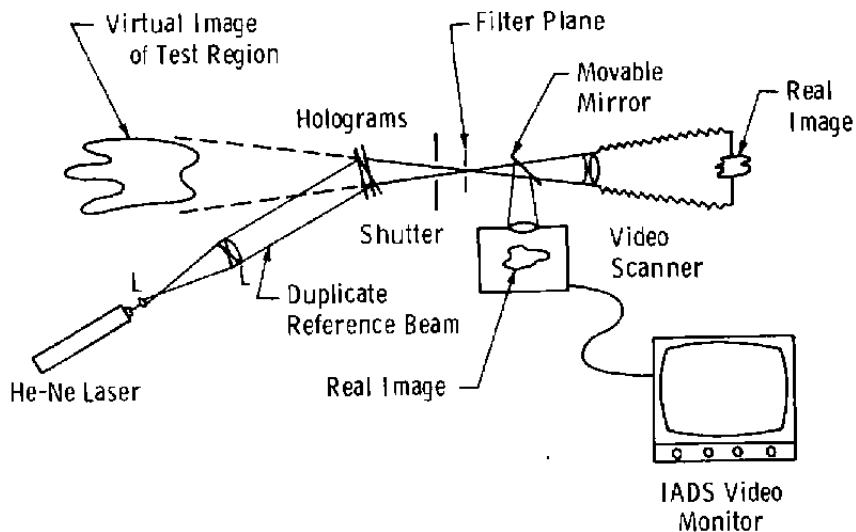


**Figure 13. Holographic reconstruction system.**

rotation with reference to the first plate. Since the sandwich holographic interferometry technique described in Ref. 8 has been adopted for all holographic recordings, separation between the two plates and the tilt adjustments originally provided on this double-plate holder are no longer utilized. The double-plate holder was modified to hold the two glass plates in contact, emulsion to emulsion. The reconstructed image is initially imaged by a scanner and displayed on a video monitor for alignment purposes. After alignment, the image can be transmitted to an Image Analyzer Digitizer System (IADS) or the TV scanner can be traversed to the side and the image recorded on 4- by 5-in. film. This reconstruction system provides for transmitted light hologram reconstructions using the shadowgraph, schlieren, or interferometric techniques. It also can be easily modified to reconstruct reflected light holograms and reflected light interferograms (Fig. 14).

#### **4.0 TRANSMISSION HOLOGRAPHIC FLOW VISUALIZATION**

Flow visualization recordings are used extensively in the VKF wind tunnels to document the flow field around models and to extract qualitative information about the flow field. The techniques available, using permanent conventional flow visualization systems, are shadowgraph and schlieren. These techniques are useful in determining the boundaries of shock waves, turbulence, boundary-layer characteristics, and density gradients. If quantitative information about the flow field is required, interferometry, pressure and/or temperature probes, or hot-wire anemometry is normally employed. Interferometry is the only one of these techniques which does not perturb the flow field. This nonintrusive characteristic makes interferometry an attractive diagnostic technique. Because of problems associated with vibrations and large windows, the use of conventional interferometry for

quantitative flow-field measurements is impractical. The transmission holographic flow visualization system described in Section 2.0 provides a means to circumvent the problems associated with conventional interferometers. Since all the information contained in the electromagnetic light wave that passes through a flow field can be recorded on a hologram, it can be recalled later under laboratory conditions to produce an interferogram. The shadowgraph and schlieren techniques can also be applied to the reconstructed wave along with many other optical processing methods (Refs. 2, 3, and 4).

#### 4.1 TRANSMISSION INTERFEROMETRY

A number of holographic techniques can be applied to flow visualization interferometry. In each of these, an unmodulated reference wave is mixed with the object wave which is passed through the flow field. The method chosen for use with the transmission holographic flow visualization system is basically the same as described in Ref. 2 along with a modified version of the sandwich holographic technique described in Ref. 8.

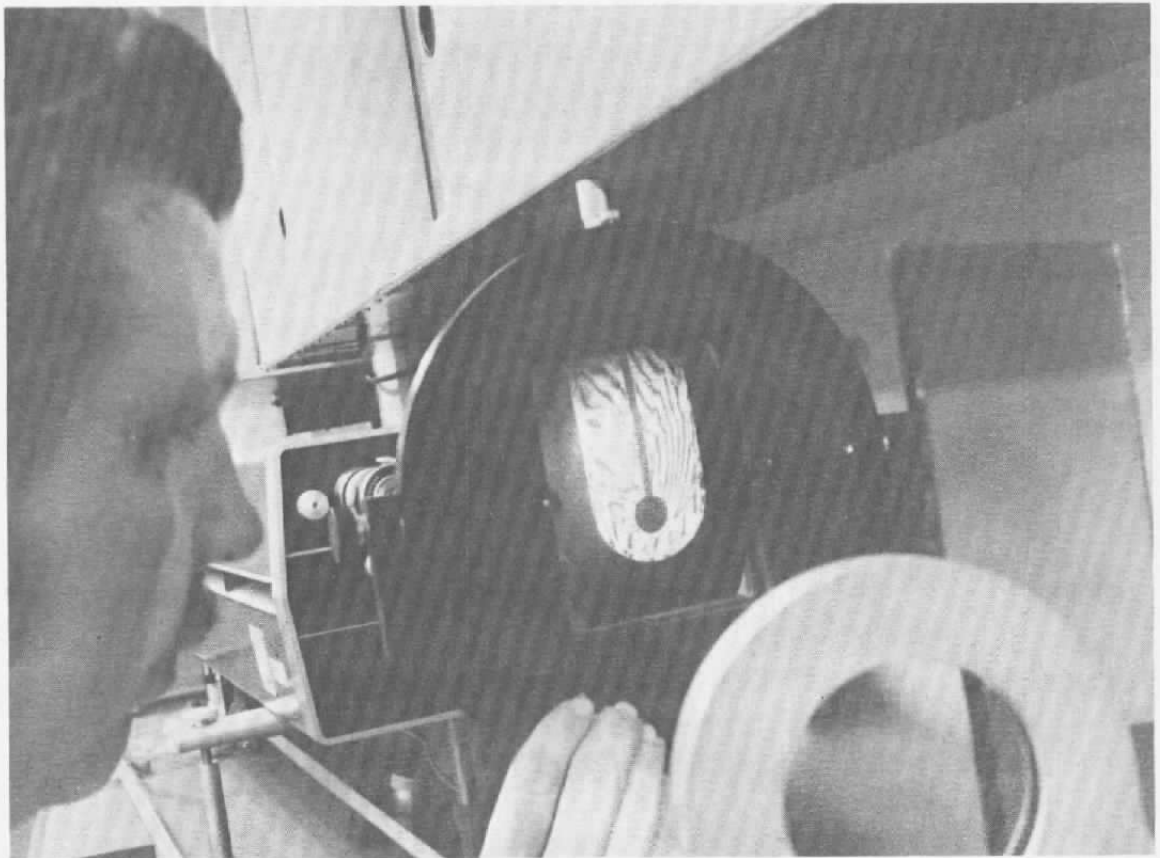


Figure 14. Diffuse reflection interferogram reconstruction.

The sandwich technique provides a simplified method of aligning two holograms for reconstruction at the same time. The reference hologram is recorded with the model removed from the wind tunnel, or, in some cases, with the model in place before the wind tunnel is started. A glass film plate with no antihalation backing is placed in the film holder with the emulsion facing away from the light beam and one plate thickness forward of the object plate position (Fig. 2). The reference hologram is recorded through the back of the glass film plate. The object plate is recorded in the normal emulsion forward position, one thickness behind the reference plate position. This arrangement is essentially the same as the sandwich technique described in Ref. 8, with the exception that the two plates are not recorded emulsion-to-emulsion. The two holograms are reconstructed emulsion-to-emulsion, eliminating the necessity of precisely aligning the distance and the angle between the two plates during reconstruction. Other aspects of the holographic interferometric technique are the same as described in Ref. 2.

Figure 15 is a typical interferogram reconstruction using this modified sandwich technique. Finite fringe interferograms are normally used for ease in data reduction although infinite fringe interferograms can be obtained with ease.

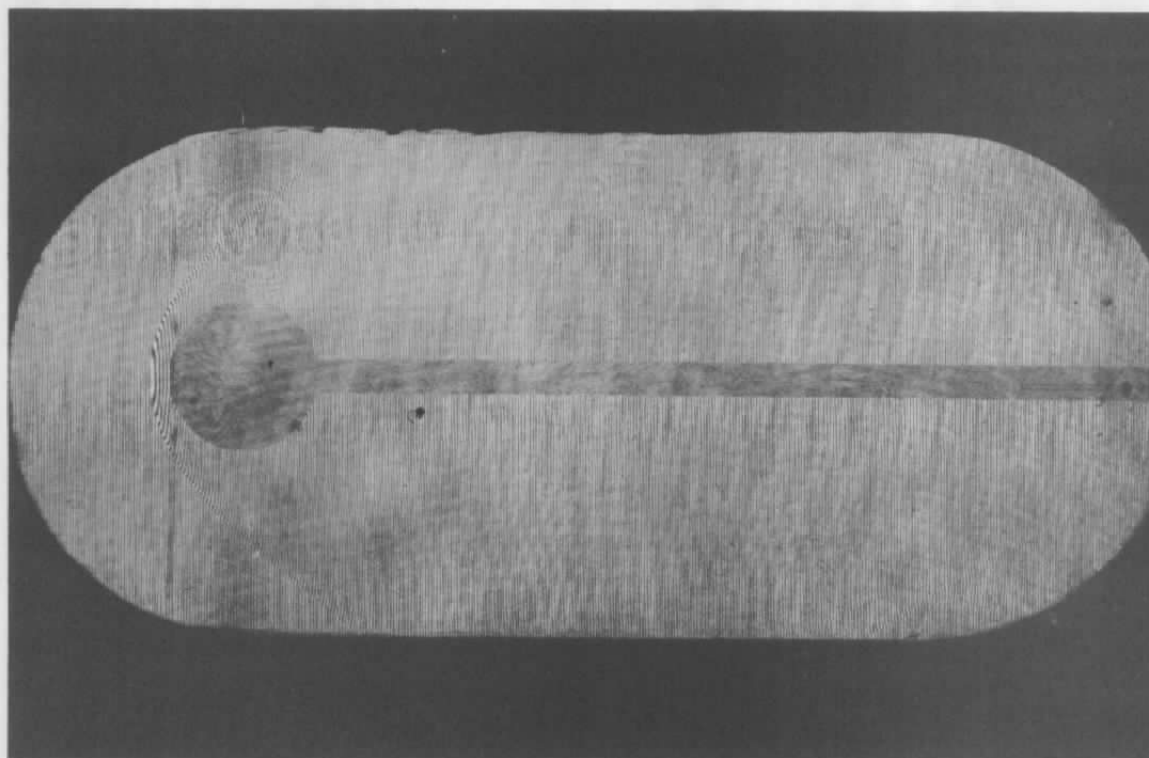


Figure 15. Interferogram reconstruction, transmitted light.

## 4.2 SHADOWGRAPH AND SCHLIEREN RECONSTRUCTION

The object hologram that was recorded through the flow field can also be reconstructed alone to obtain shadowgraph and schlieren recordings. A shadowgram of the flow field is obtained simply by defocusing the flow field as with conventional refocused shadowgraph photography (Fig. 16a). Schlieren flow visualization is obtained with the flow field focused and a knife edge inserted into the image of the laser light source and adjusted for the sensitivity desired (Fig. 16b). These two techniques do not replace the effectiveness of conventional flow visualization, particularly when large volumes of recordings are to be made. However, they are useful in supplementing the information obtained from interferograms reconstructed from the same hologram.

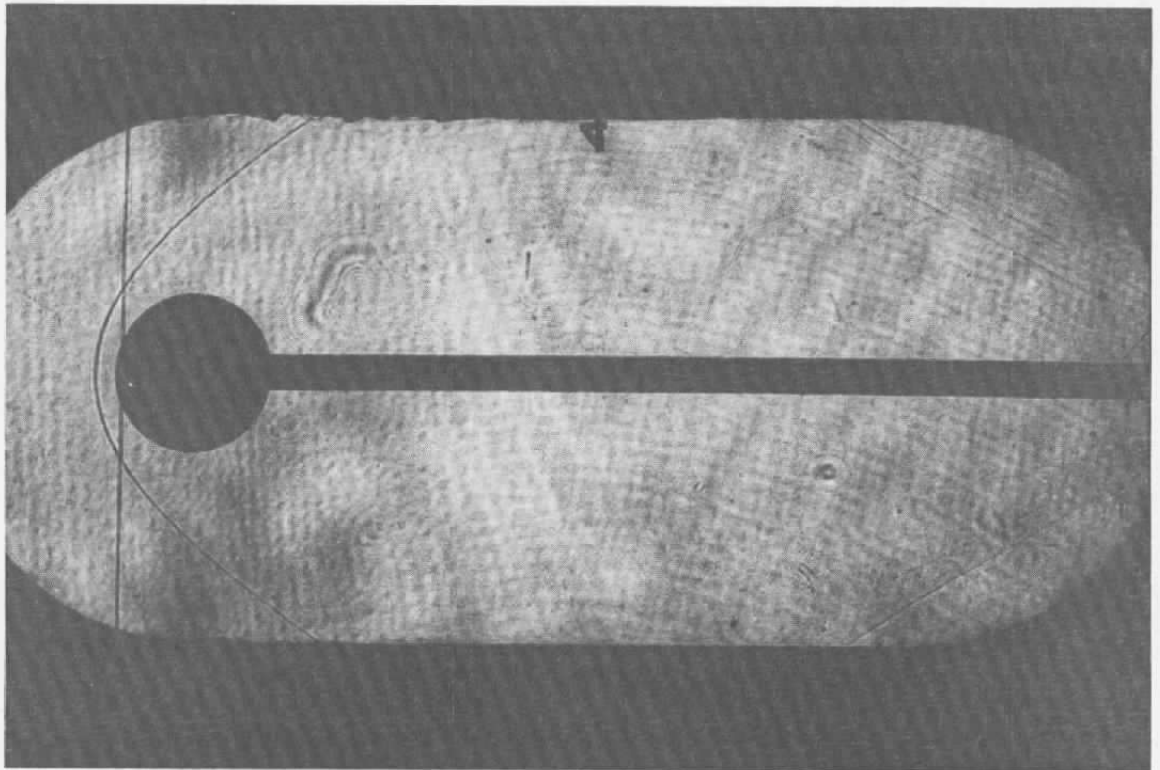


Figure 16a. Shadowgraph reconstruction.

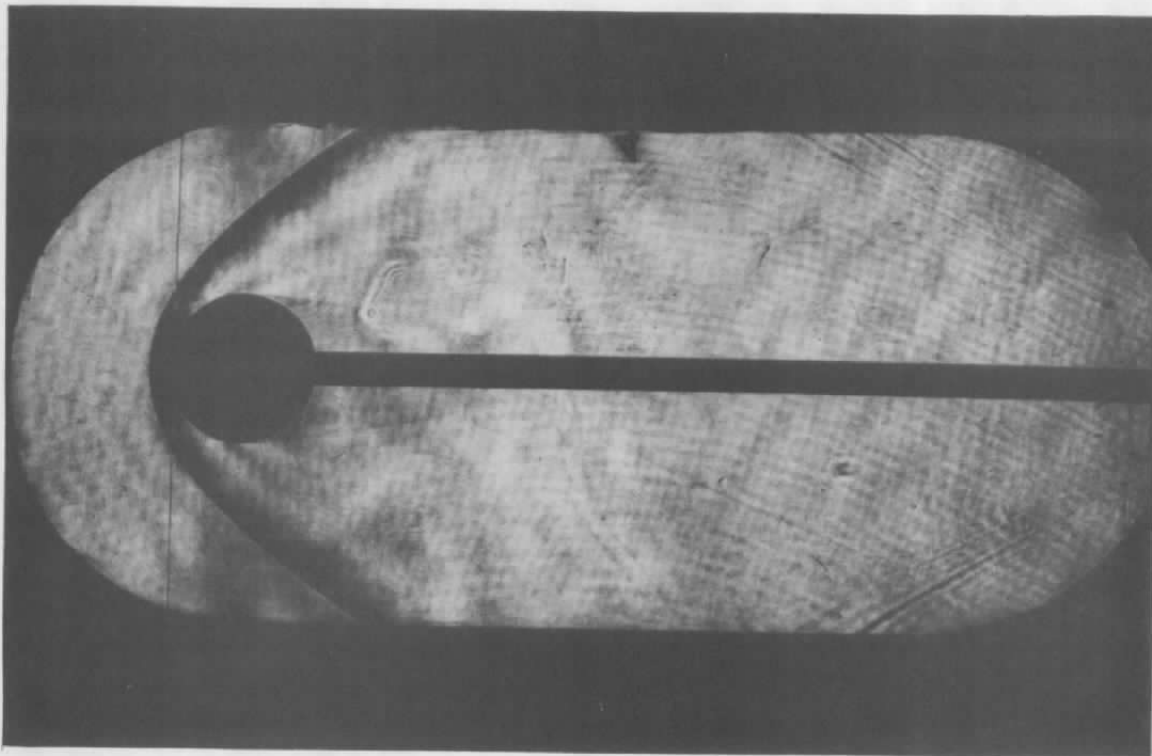


Figure 16b. Schlieren reconstruction.

## 5.0 DIFFUSE REFLECTION HOLOGRAPHIC FLOW VISUALIZATION

Experiments using diffused reflected light interferometry have led to the conclusion that this type of interferometry has only one significant advantage over the transmitted light interferometry for wind tunnel testing. Although the diffused reflected light interferometric fringes are three-dimensional, which permits observation of a flow field from different angles, the fringes are (1) localized in space, (2) difficult to reconstruct, and (3) generally have lower contrast and resolution than fringes produced with transmitted light. However, the use of diffused reflected light interferometry provides the unique capability of observing flow fields in cavities, corners, or in front of opaque surfaces. As an example, the flow field at the intersection of an aircraft wing and its fuselage can be observed. This is not possible with transmitted light interferometry since this area is always in the shadow of the opaque wind tunnel model.

### 5.1 DIFFUSE REFLECTION INTERFEROMETRY

Initial experiments in the laboratory while developing this technique were directed toward determining the effects of optical system and model movement that can be expected

around large high-speed wind tunnels. The breakthrough that made this technique possible was the ability to record a reflected diffuse light reference hologram and at a later time record a reflected diffuse light data hologram of a disturbed flow field and realign them with the accuracy required to produce interference between the two reconstructed wave fronts. Unlike transmitted light interferometry, reflected light holograms must be aligned to within a few wavelengths before fringes become visible. The ability to achieve the required accuracy in the alignment of holograms made in a vibrating environment was heretofore believed to be beyond the present state-of-the-art. The implementation of the sandwich holographic technique described in Section 4.1 made this possible. The technique is basically a method of recording two holograms in such a way that they can be reconstructed with their film emulsions in contact. This eliminates the need for spacing and angular adjustment between the two holograms as required by the technique reported in Ref. 3.

For experiments in the laboratory, a typical wind tunnel model was painted with Scotchlite reflective paint and an open-air 10-kv spark was discharged just below the wing root to provide a disturbance in the air (Fig. 8). The interferometric fringes resulting from density changes of the air can be observed against the opaque surface of the model (Fig. 17). Similar interferograms were made to determine the effects of optical system and model movement between the reference and data hologram recordings. Although these motions are not well defined under wind tunnel operating conditions and would be difficult to reproduce in the laboratory, the results of the experiments indicated that the problem is not insurmountable. An attempt to produce a double-plate diffuse reflected light interferogram in the VKF Tunnel A was unsuccessful because of gross movement of the breadboard optical system and a change in model attitude (caused by aerodynamic loading) of approximately 1 deg between the reference and data hologram recordings. Since compensation for a 15-min angular model movement was successful in the laboratory, it is expected that the operational reflected light holographic system with its rigidly mounted optical components will solve this problem. More experimental work with this system under tunnel operating conditions is required.

Another diffuse reflected light interferometric technique, double-pulse interferometry, which utilizes the double-pulse capability of the pulsed ruby laser has possible applications in wind tunnel testing. Two holograms are recorded on the same film plate with a time separation of from 10 to 500  $\mu$ sec. The interferometric fringes characterize changes in the flow field that occur between the two pulses. This technique may be useful in observing turbulence and determining the time scale or velocity of the turbulent cells by varying the pulse separation. An experiment was conducted in the VKF Tunnel A to verify the operational capabilities of the Diffuse Reflected Light Holographic System using this technique. A 15- by 20-cm panel on the side of the AEDC Inlet/Throttle metering model was

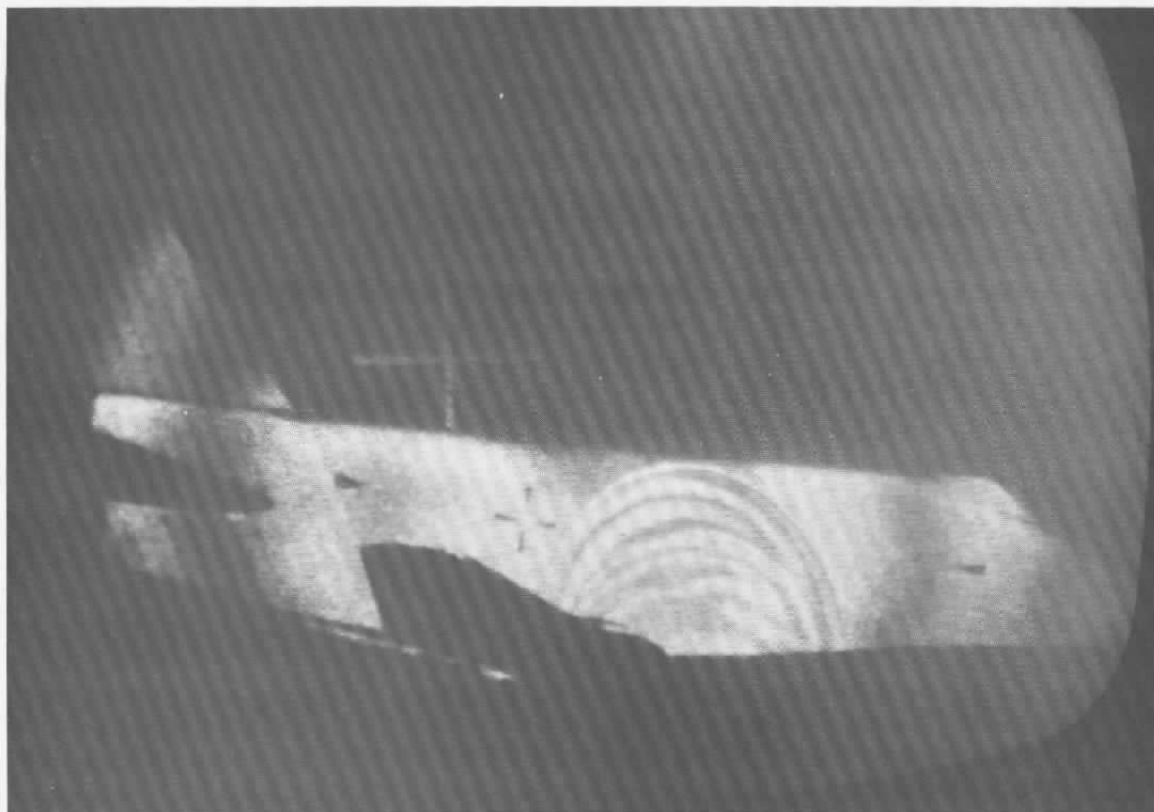


Figure 17. Diffused reflected light interferogram, double plate.

painted with Scotchlite to provide a highly reflective background in an area of known turbulence (Fig. 18a). Double-pulse, time-difference reflected light interferograms of the turbulent flow field on the side of the model were recorded with a  $50\text{-}\mu\text{sec}$  pulse separation (Fig. 18b) and with a  $200\text{-}\mu\text{sec}$  pulse separation (Fig. 18c). The increase of turbulent cells over the longer time span can be observed. Analysis of this type of interferometric data in terms of turbulence frequency and velocity requires further study.

## 6.0 AUTOMATED INTERFEROGRAM ANALYSIS AND DATA REDUCTION

In the case of finite fringe interferometry the magnitude of the fringe shifts can be related to the variation in static density. Therefore, accurate measurements of fringe coordinates must be made. Traditional means of making fringe shift measurements by hand or by semiautomatic film readers are time consuming; subjective decisions must be made using the human eye. Since interferograms reconstructed from holograms are typically noisy because of the use of coherent light, the centerlines of the fringes are more difficult to locate than with conventional monochromatic light interferograms where the intensity profile

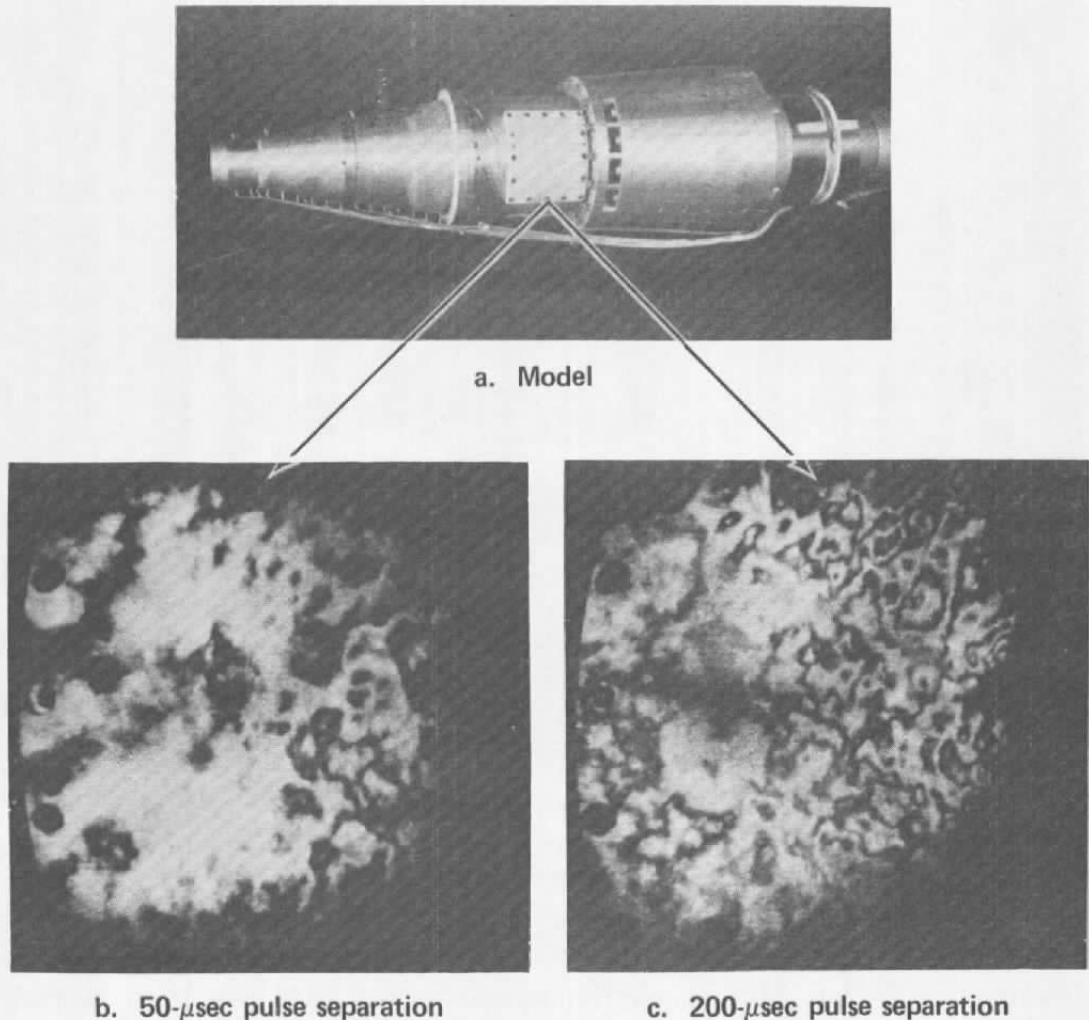


Figure 18. Reflected light interferogram, time difference.

perpendicular to the fringes is sinusoidal in nature. Therefore, when utilizing an automatic means of locating fringe centers, it is desirable to first enhance the images of the fringes before making a determination of the centerline location. Recent advances in digital image analysis hardware and development of new digital image analysis techniques have provided the technology required for making consistent interferometric fringe measurements and suppression of noise for acceptable accuracy in fringe measurements.

### 6.1 IMAGE ANALYZER-DIGITIZER SYSTEM

The Image Analyzer-Digitizer System (IADS) (Fig. 19) uses a video scanner with high uniformity in its photometric response and geometric accuracy to scan the interferogram image and subsequently digitize it into a 640 horizontal by 480 vertical picture element



Figure 19. Image analyzer-digitizer system.

(pixel) array (Ref. 9). Each of the 307,200 pixels is assigned a gray level value between 0 and 255, 0 being the darkest and 255 being the lightest. The scanner is interfaced to a Spatial Data Systems EyeCom digitizer which digitizes the image from the scanner in either a linear or logarithmic mode. The digital image is then recorded on a magnetic disk under control of a Digital Equipment Corporation (DEC) PDP-11/04 minicomputer (Fig. 20). The EyeCom digitizer combines the basic features of an intelligent alphanumeric terminal, graphics display, video monitor, and a joystick cursor and keyboard for operator interaction with the computer. The minicomputer is also interfaced to a computer for further data reduction which cannot be handled by the minicomputer. Two magnetic disk drives are available for software storage and also provide picture files for up to 12 images. Output devices for the image analyzer system include a film recorder, printer, plotter, and a color video monitor.

## 6.2 INTERFEROMETRIC RECONSTRUCTION AND DIGITIZATION

The holographically recorded interferogram is reconstructed using the reconstruction system described in Section 3.0. The interferogram is imaged directly into the scanner and transmitted directly to the EyeCom digitizer (Fig. 19). The interferometric image is digitized from four to eight times and then averaged to reduce effects of electronic noise.

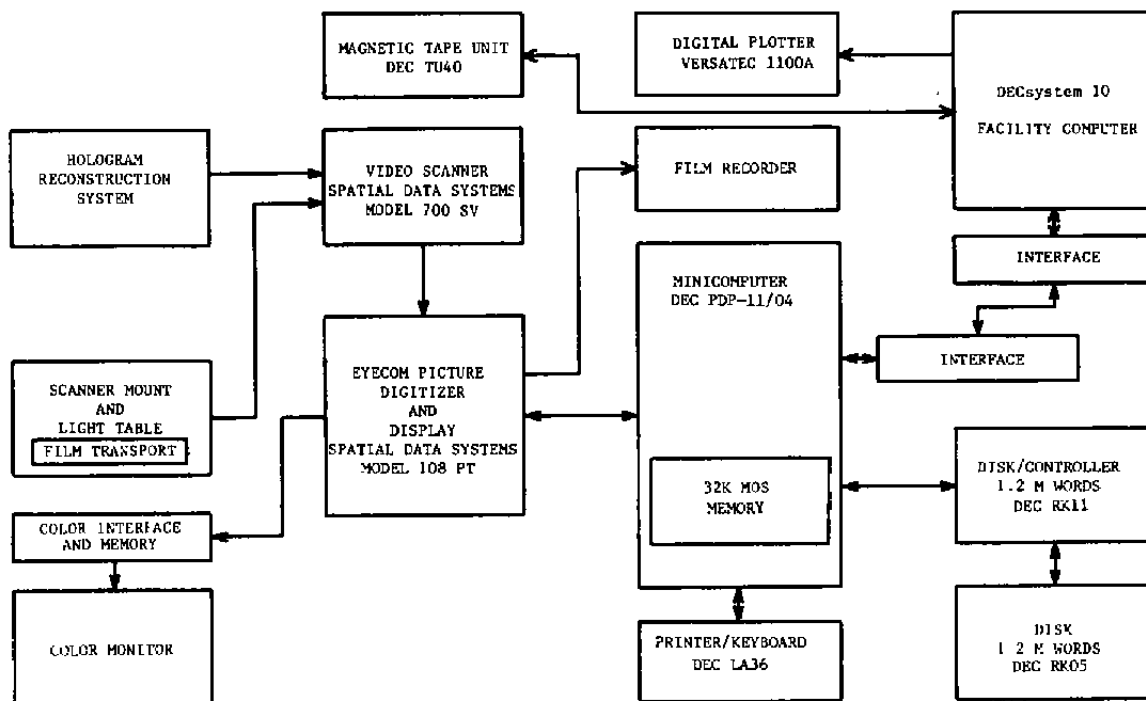


Figure 20. Schematic of image analyzer-digitizer system.

### 6.3 INTERFEROMETRIC FRINGE MEASUREMENTS

In order to process the information contained in an interferogram to obtain static density distributions in a flow field, the finite fringe pattern of the flow field must be converted into an accurate digital format, i.e., the coordinates of the fringe pattern and the assigned fringe number must be listed. Past experience has shown that manually reading and recording this amount of data will, in most cases, result in errors which will compromise the final result. Obviously, some judgment must be used in selecting the center of a fringe line. The error incurred in the manual location of this line center is probably  $\pm 5$  to 10 percent of the nominal fringe spacing. A problem also exists in the manual reading of interferograms with regard to identification of the number assigned to a particular fringe.

The following discussion will illustrate the automated technique which is available for analyzing a typical interferogram. An axisymmetric flow-field pattern was chosen as an example case for consideration. The interferogram shown in Fig. 15 represents the flow field produced by a sphere (2.854-cm-radius), strut supported, in a Mach number 2.5 supersonic stream. The undisturbed free-stream density upstream of the bow shock wave was 0.481 mg/cc. The analysis will consist of defining the local density distribution along a line in the plane at a distance of 14.4 percent of the sphere radius from the sphere nose as shown in Fig. 21 and denoted as the datum line.

Initially, the interferogram shown in Fig. 15 was digitized in terms of discrete points (pixels) in the image field and each pixel was assigned a gray level between 0 and 255, producing the enlarged digitized image shown in Fig. 21. A known dimension such as the sphere radius can be used to establish the scale factor (pixels per unit length). In this particular case, the scale factor was 68.02 pixel/cm. The image processor is then used to define the fractional fringe shift distribution along the datum line using the computer program "FRINGE 2." A listing of this program is given in Appendix A. Using an arbitrary, but sequential fringe numbering system, the fringe values adjacent to the datum line are interpolated to define the fractional fringe shift variations along the datum line.

The following neighborhood averaging algorithm is used to eliminate high frequency noise of the gray level  $[G(I)]$  distributions along a pixel  $[I]$  column perpendicular to the datum line where  $N$  is the filtering segment length in pixels. The operator can determine the effectiveness of the filtering operation from a cursory inspection of the interferogram displayed on the video monitor. Further filtering can be applied if required for proper fringe continuity interpretation by the program (see Fig. 22).

This procedure is repeated for each datum line until the fringe distribution is defined from the body to the free stream. The results of such analysis are shown in Fig. 23. These data are then transmitted to the DEC system 10 computer for the remainder of the analysis (Appendix B).

#### 6.4 INTERFEROMETRIC DATA REDUCTION

The right and left sides of the fringe distribution shown in Fig. 23 were evaluated with a slight shift in the fringe number system; therefore, the distribution on the right needs to be shifted by one fringe number (ordinate axis) relative to the distribution on the left. This causes the fringe distributions on the right and left side to be consistent and directly comparable to each other. The shifted results are shown in Fig. 24. The next step is to normalize the distribution relative to the free-stream fringe line which becomes the reference for defining the net shift in a fringe line caused by the disturbance produced by the sphere flow field. The magnitude of the reference fringe shift in the free-stream area of the interferogram varies along a line which is parallel to the datum line as suggested in Fig. 24. This distribution is normalized by subtracting the reference fringe line from the flow-field fringe shift distribution to produce the result shown in Fig. 25.

In this case, for symmetrical flow fields, the fringe shift results from the right and left sides of the image field being correlated as a function of the square of the radial coordinate as shown in Fig. 26. A least square curve fit of these results in three discrete segments is used

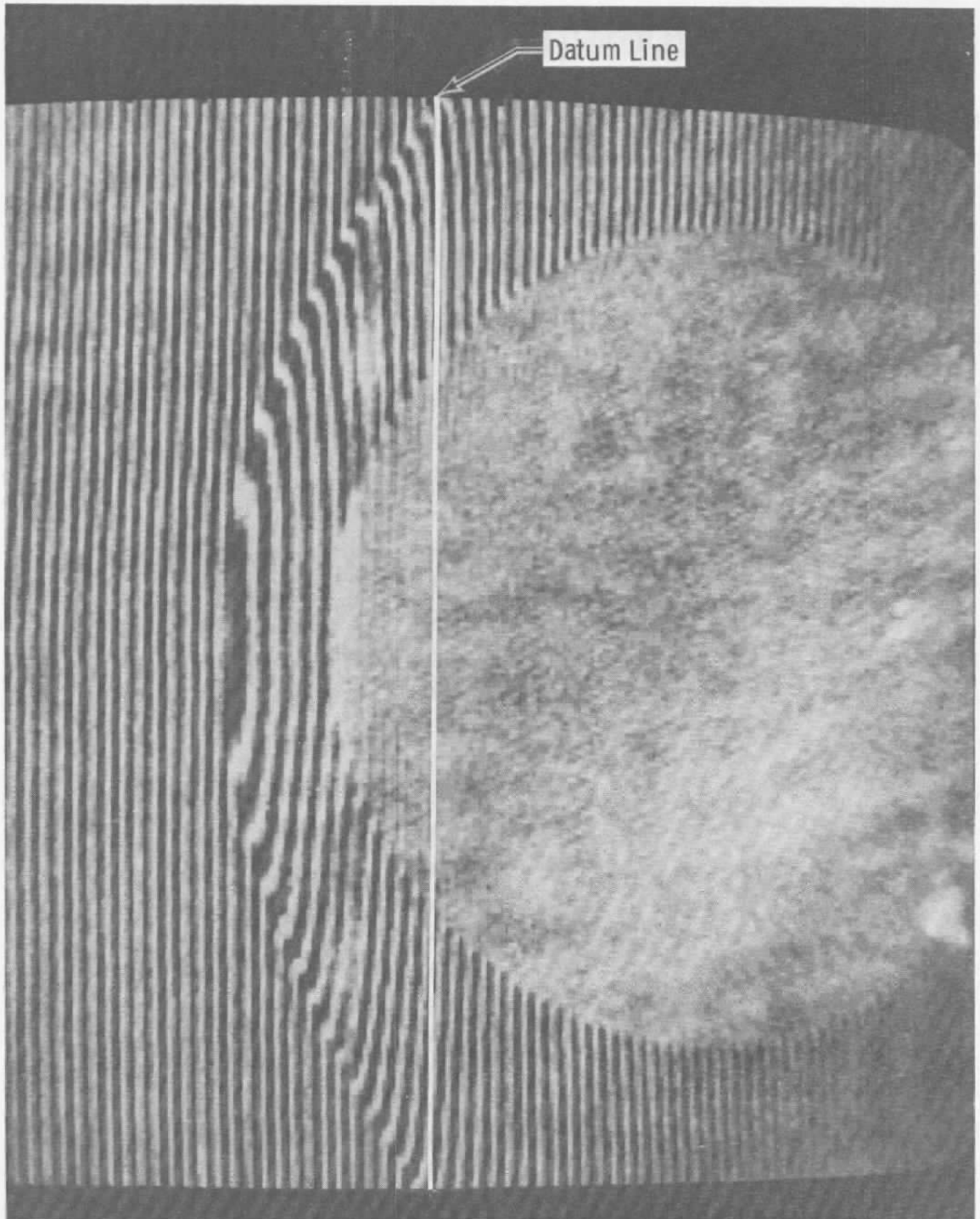


Figure 21. Digitized image of interferogram.

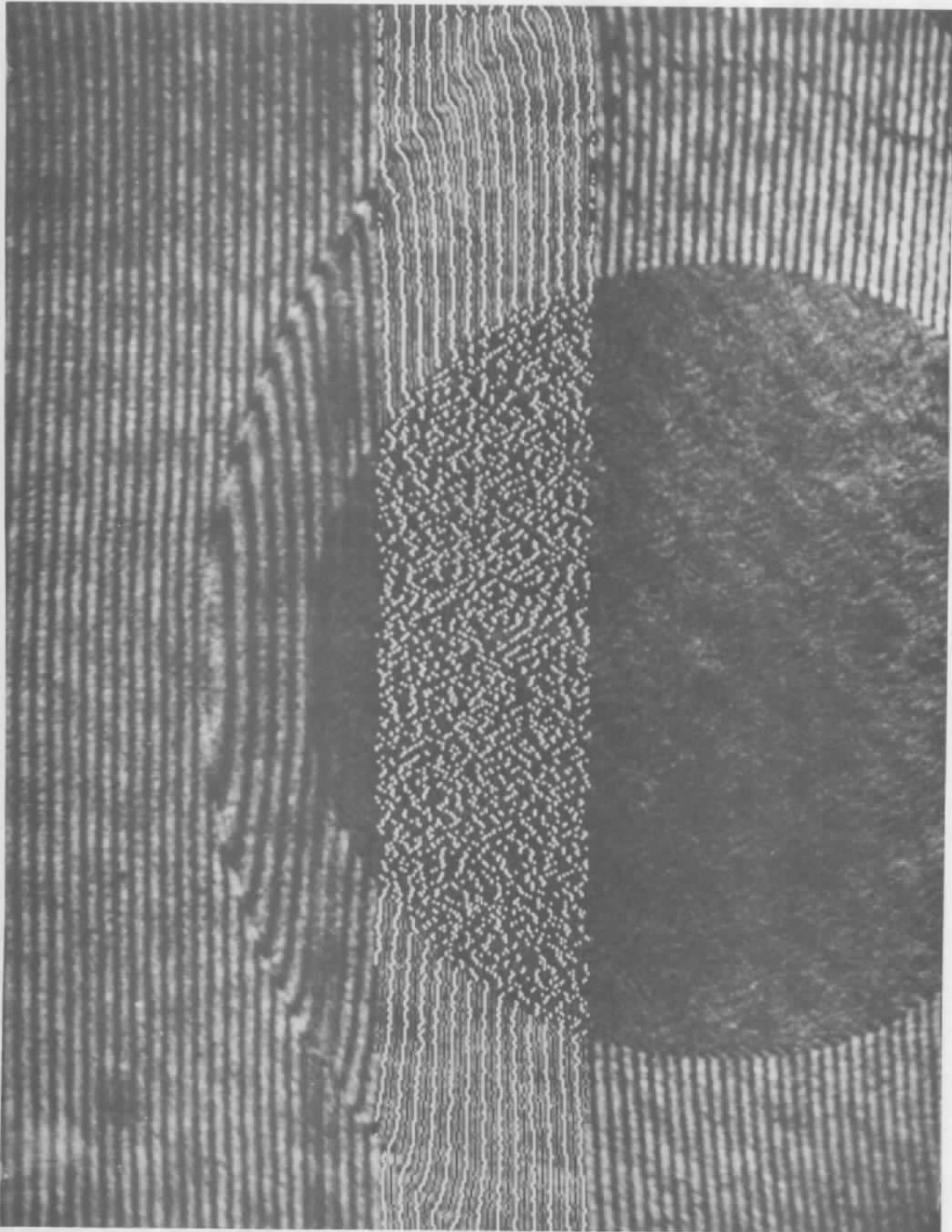


Figure 22. Fringe centerline tracking.

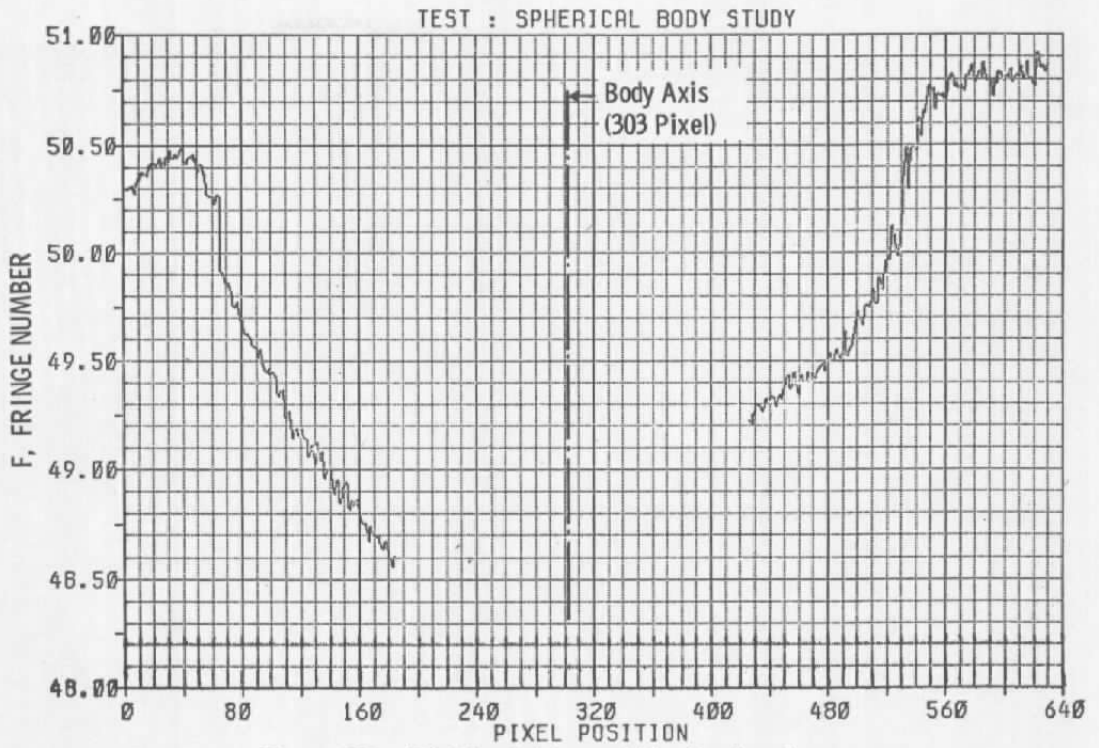


Figure 23. Digitized fringe shift distribution.

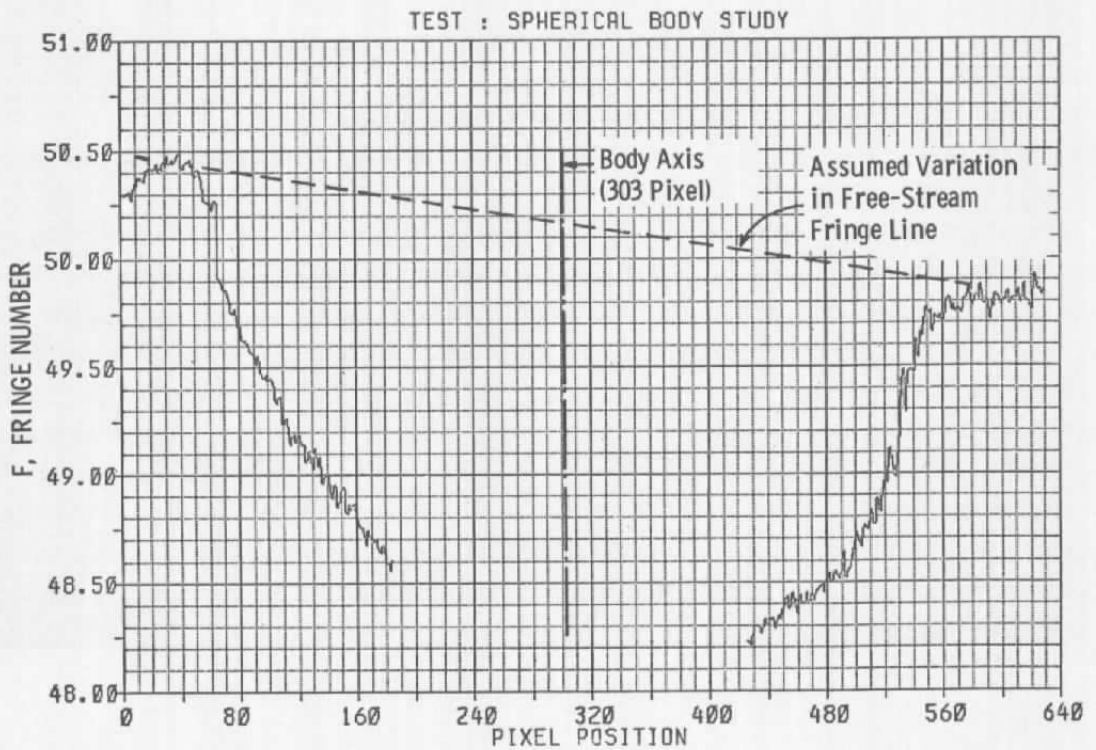


Figure 24. Corrected fringe shift distribution.

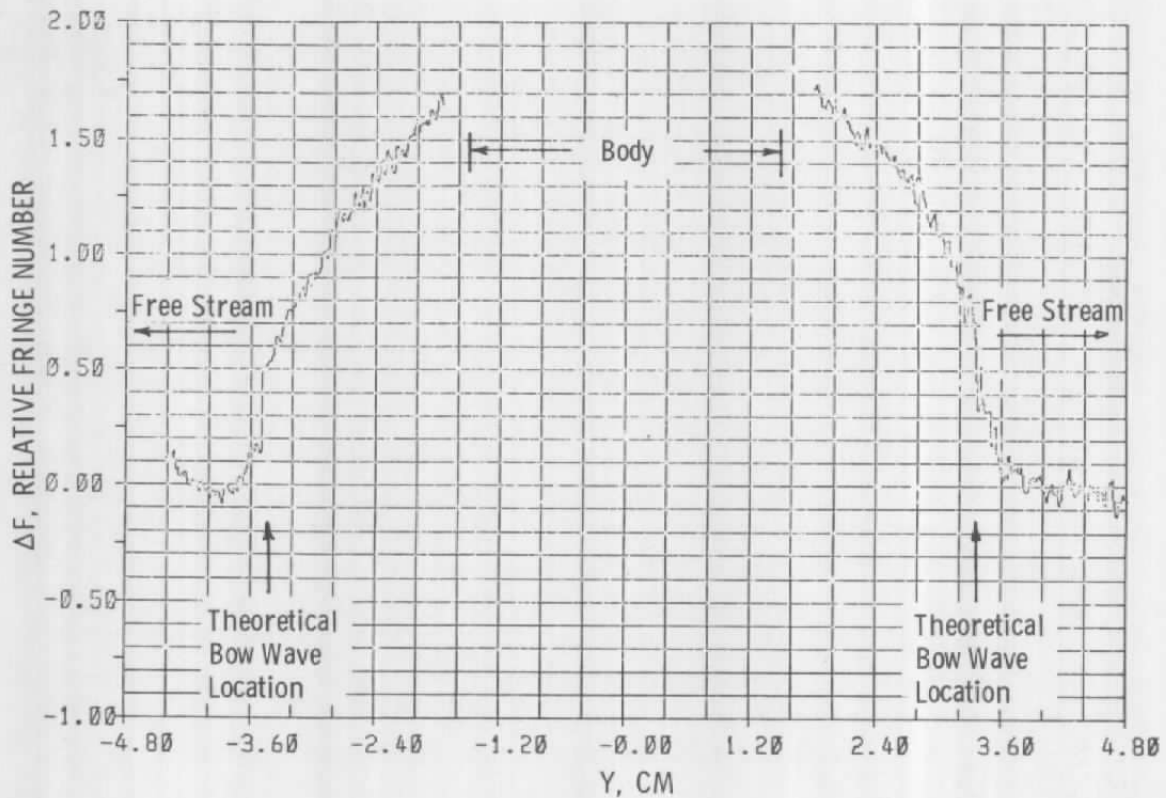


Figure 25. Normalized fringe shift pattern.

to establish a continuously smooth variation of the fringe shift with radial (Y) position which is plotted in Fig. 26. The resulting curve fit of the fringe data is presented in Fig. 27.

The fringe shift distribution is defined continuously through the region occupied by the body which, although physically meaningless, is a useful scheme for minimizing the noise in the numerical computations. The flow-field density distribution from the body to the bow shock wave as inferred from the curve fitted fringe shift information in Fig. 27 is presented in Fig. 28. The analysis of Van Houten (Ref. 10) was used in this axisymmetric interferometric analysis. Included in the figure is a theoretical estimate of the density distribution obtained from the analysis presented in Refs. 11 and 12. For 301 data points the interferometry program takes about 38 sec of CPU time on the DEC system 10 computer. This includes the time to drive the Versatec 1100A printer-plotter. Plots of expanded fringe, refractive index, and flow-field density ratios are obtained during the program. A printout of calculated values is also obtained.

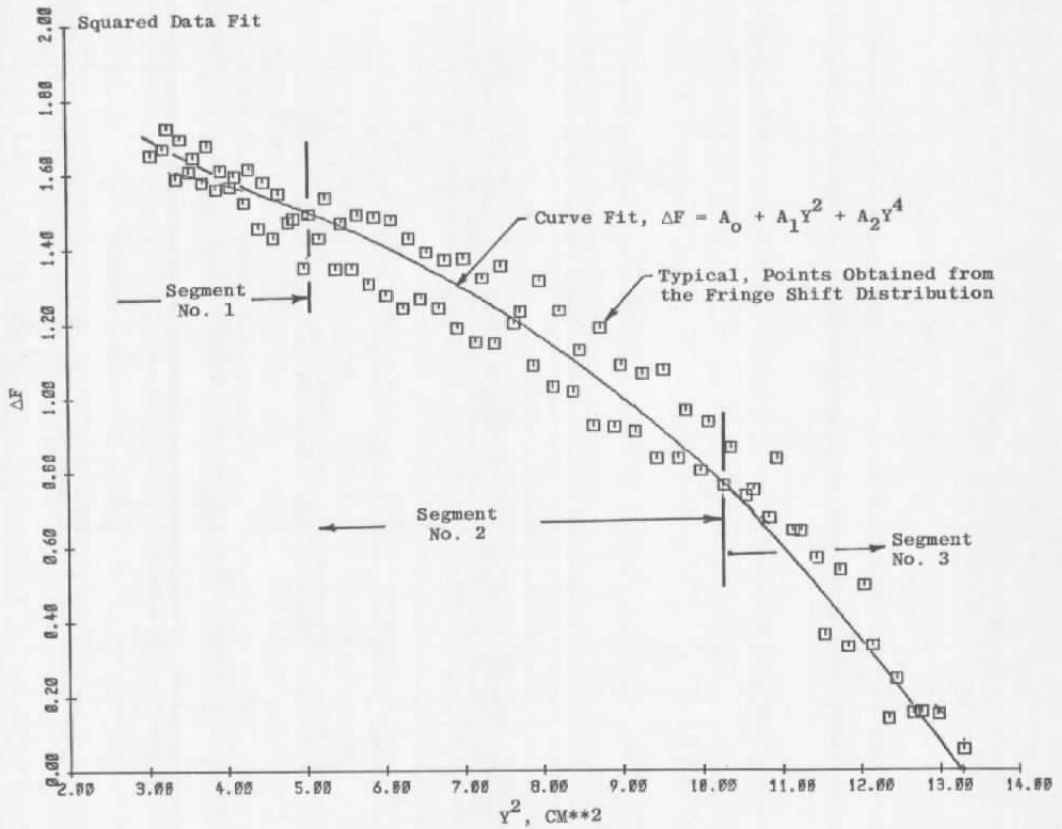


Figure 26. Correlation of fringe shift pattern.

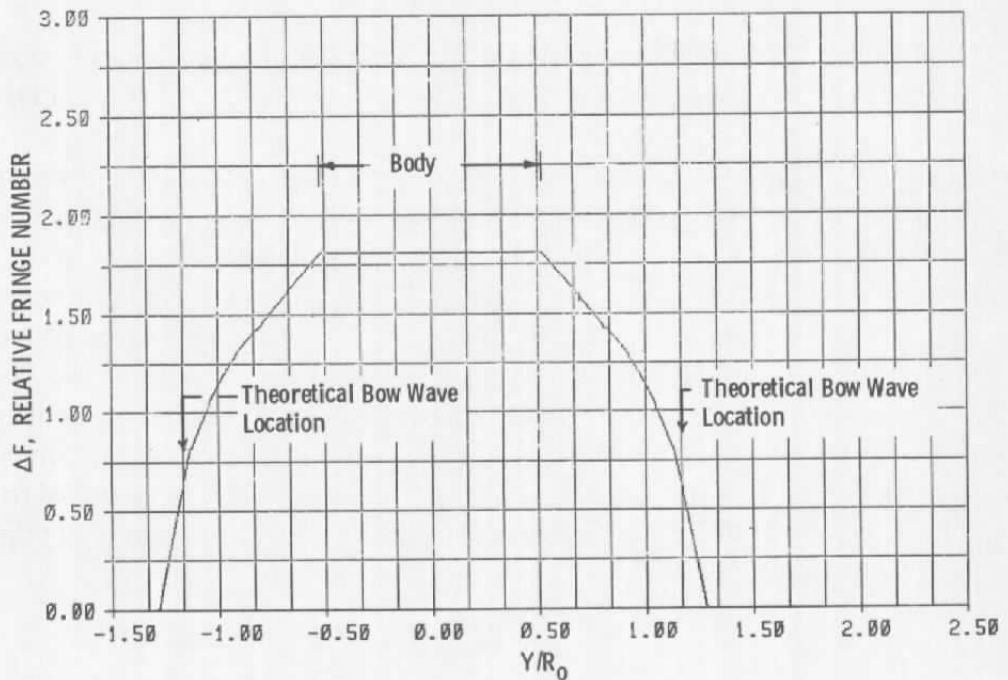


Figure 27. Curve fit of the fringe shift data distribution.

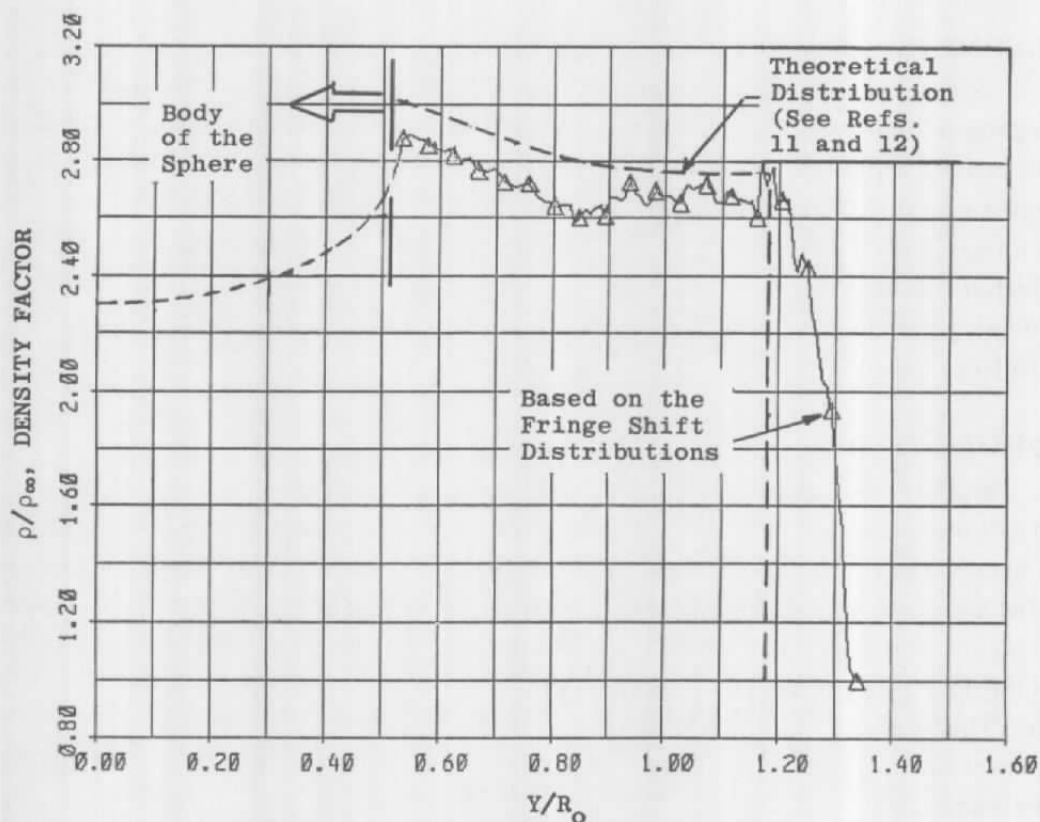


Figure 28. Density distribution in the flow field of a sphere.

## 7.0 IMAGE ANALYSIS APPLICATION TO OTHER AERODYNAMIC TESTING TECHNIQUES

The application of image analysis using the IADS to other aerodynamic testing techniques was investigated to replace the traditional means of extracting information manually from photographic images (i.e., using the human eye and subjective decisions) with computer assisted analysis and digital data reduction. Images contain a wealth of information that can be extracted and analyzed by the minicomputer providing quantitative measurements along with traditional visual observation of the image. The images and digital data can (1) be complemented with graphic displays, (2) provide graphic analysis of certain data inherent in the image, and (3) provide alphanumeric data to supplement the image presentation with written titles and other supplementary data. Unique software has been developed for the IADS for application to analyzing images using several aerodynamic testing techniques. This has enhanced the usefulness of the photographic data.

## 7.1 GEOMETRIC AND PHOTOMETRIC MEASUREMENTS

A program entitled "LOOK" was developed for initial interactive image analysis and also to provide inputs required for specific image analysis techniques. This program includes the software needed to make geometric and photometric corrections and measurements from images and to digitally correct the scanner sensitivity to the D-log-E curve of the film on which the image is recorded. After this calibration has been made the gray level values, or film density values, are linear with respect to the light intensity that was incident upon the film to form the image.

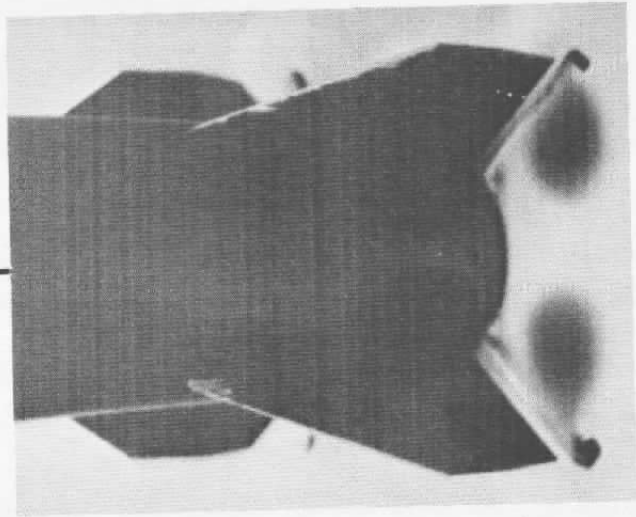
## 7.2 PHOTOMETRIC CORRECTIONS

When making conventional photometric measurements from photographic images, one must assume that the subject was evenly illuminated for these measurements to be accurate. In other cases the unevenness of paint on the subject or dirt smudges could also reduce the accuracy of the photometric data. Software was developed to compensate for these irregularities by using information obtained from a photographic tare to normalize the data image. This technique was used with the vapor screen image shown in Fig. 29a to compensate for the Gaussian intensity profile of the vapor screen caused by the use of a helium-neon laser as the light source. A photographic recording was made of the intensity profile of the vapor screen, and the variation across the image area was digitized and stored on disk. The data image was then recorded in registration with the tare image and the final corrected image was obtained by subtracting the tare from the data image.

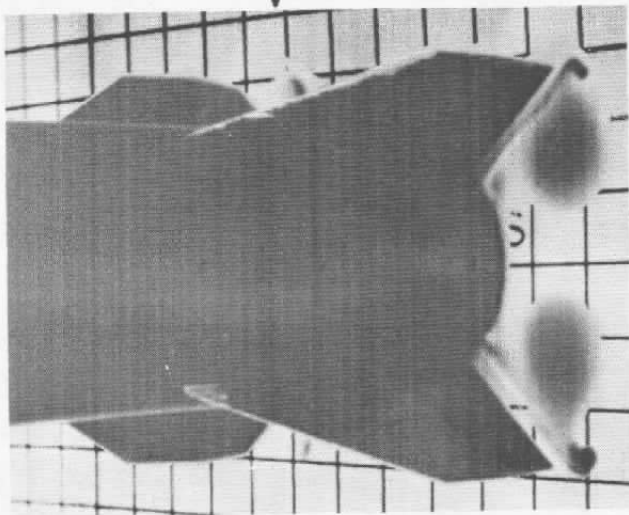
## 7.3 CAMERA PERSPECTIVE MODIFICATION

Software has been developed for the IADS to modify the camera perspective of a two-dimensional plane image. As an example, images obtained using the vapor screen technique of flow visualization are normally recorded with a camera located outside of the wind tunnel test section, usually at an angle from 30 to 60 deg from the vapor screen plane (Fig. 29a). Even though the vapor screen plane forms a two-dimensional image, this oblique camera perspective produces an oblique view of the vapor screen which makes geometric measurements difficult. To illustrate this technique a 1-in.-square grid was placed in the plane of a vapor screen and photographed with a camera-vapor screen angle of 45 deg. The resulting grid image was digitized and added to the original digitized vapor screen image (Fig. 29b). The undesirable oblique perspective of the vapor screen plane can be noted from the converging of the originally horizontal lines. In this case it is desirable to have a normal perspective of the vapor screen plane. Using the IADS, the camera perspective was changed

Grid Added

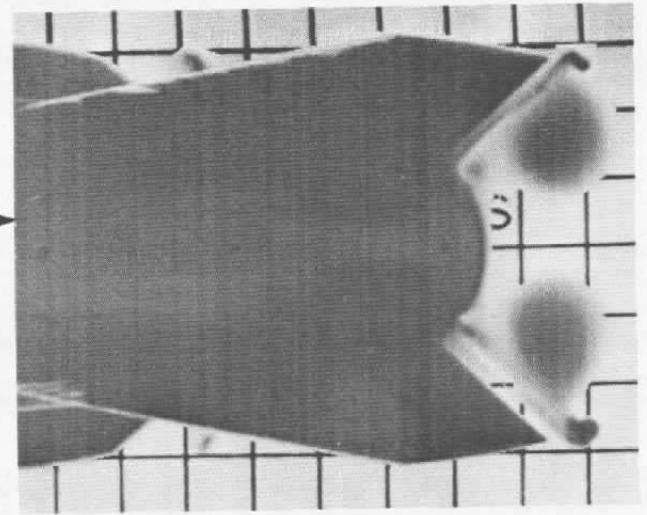


a. Digitized vapor screen image



b. Oblique perspective

Perspective Normalized



c. Normal perspective

Figure 29. Oblique camera perspective correction.

from oblique to a normal one and the results are shown in Fig. 29c. Accurate geometric measurements can now be made from this corrected vapor screen image by operator interaction with the IADS.

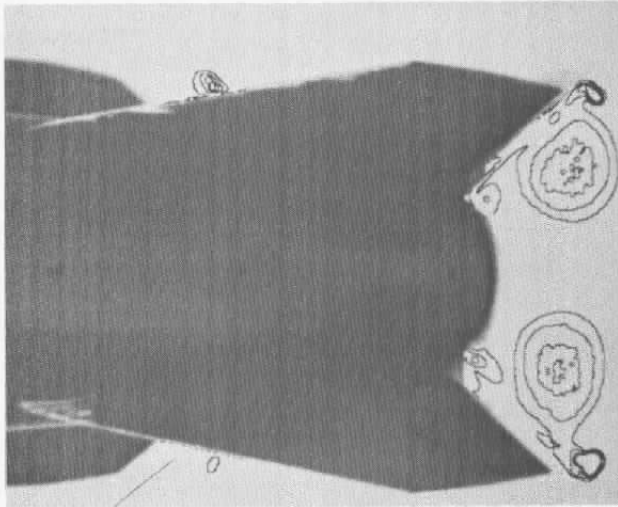
#### **7.4 PHOTOMETRIC DATA PRESENTATION**

Photometric measurements made from vapor screen images are useful in obtaining quantitative data. After the image has been corrected for the nonlinear sensitivity of the photographic film (Section 7.1) and variations in light source intensity (Section 7.2), particle distributions and flow-field densities can be inferred from vapor screen images. Using the IADS, fog particle distribution in the vapor screen can be depicted (1) by using image enhancement techniques to produce equal density contour lines (Fig. 30a), (2) by density slicing which reduces the optical density levels to fewer equally spaced levels (Fig. 30b), or (3) by equal density contouring with up to 32 colors. The eye of the vortices, as opposed to their geometric centers, can also be located using density gradient and vector averaging techniques. The coordinates of each vortex eye with respect to the model are thus determined. The location of the vortex eyes is shown by the white crosshairs in Fig. 30b.

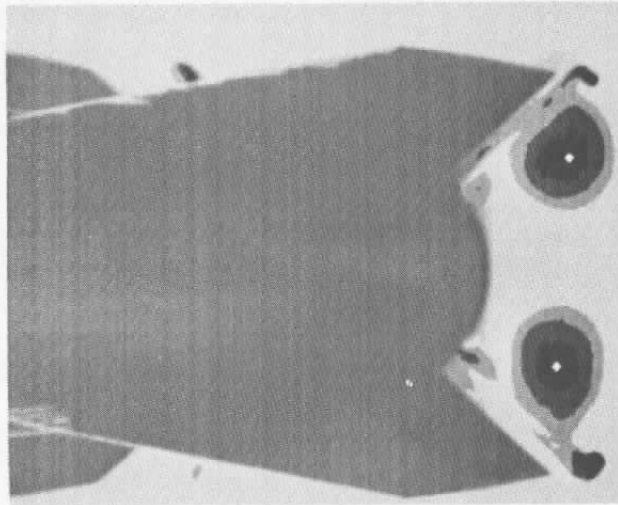
A printout of the digital photometric data can be provided by the IADS for visual and numerical analysis. The gray level values of the lower vortex are shown in Fig. 31. This printout was limited to every other pixel (one-half spatial resolution) in the interest of clarity and reduction in size for publication. The digital image data can also be transmitted to the DEC system 10 computer for numerical analysis beyond the capability of the DEC PDP-11/04 minicomputer, for recording on magnetic tape, for archival storage, or for producing line plots.

### **8.0 CONCLUSIONS**

The development, design, and fabrication of operational holographic flow visualization systems provide a new method at the AEDC for obtaining quantitative data pertinent to the flow field around models in large supersonic and hypersonic wind tunnels. These systems are now considered to be operational and can be applied to a large number of flow diagnostic problems. Improvements made in pulsed ruby laser technology have improved the quality of pulsed holographic recordings, but significant advantages over conventional flow visualization techniques for qualitative observations have not been realized. By automating the analysis of interferometric images and reducing the numerical data with computers, the use of interferometry for making diagnostic measurements which do not perturb the flow field will be a viable alternative to pitot tube and hot-wire measurements in future aerodynamic testing. Possible applications of image analysis techniques in aerodynamic testing are numerous.



a. Equal density contour lines



b. Density slicing and vortex eye centers  
Figure 30. Equal density contouring.

```

ENTER COMMAND
**** IFF = 1
ENTER COMMAND
ENTER L COL, U ROW, R COL, L ROW, INCC-INCR 1&1
446,247,533,386,2,2

```

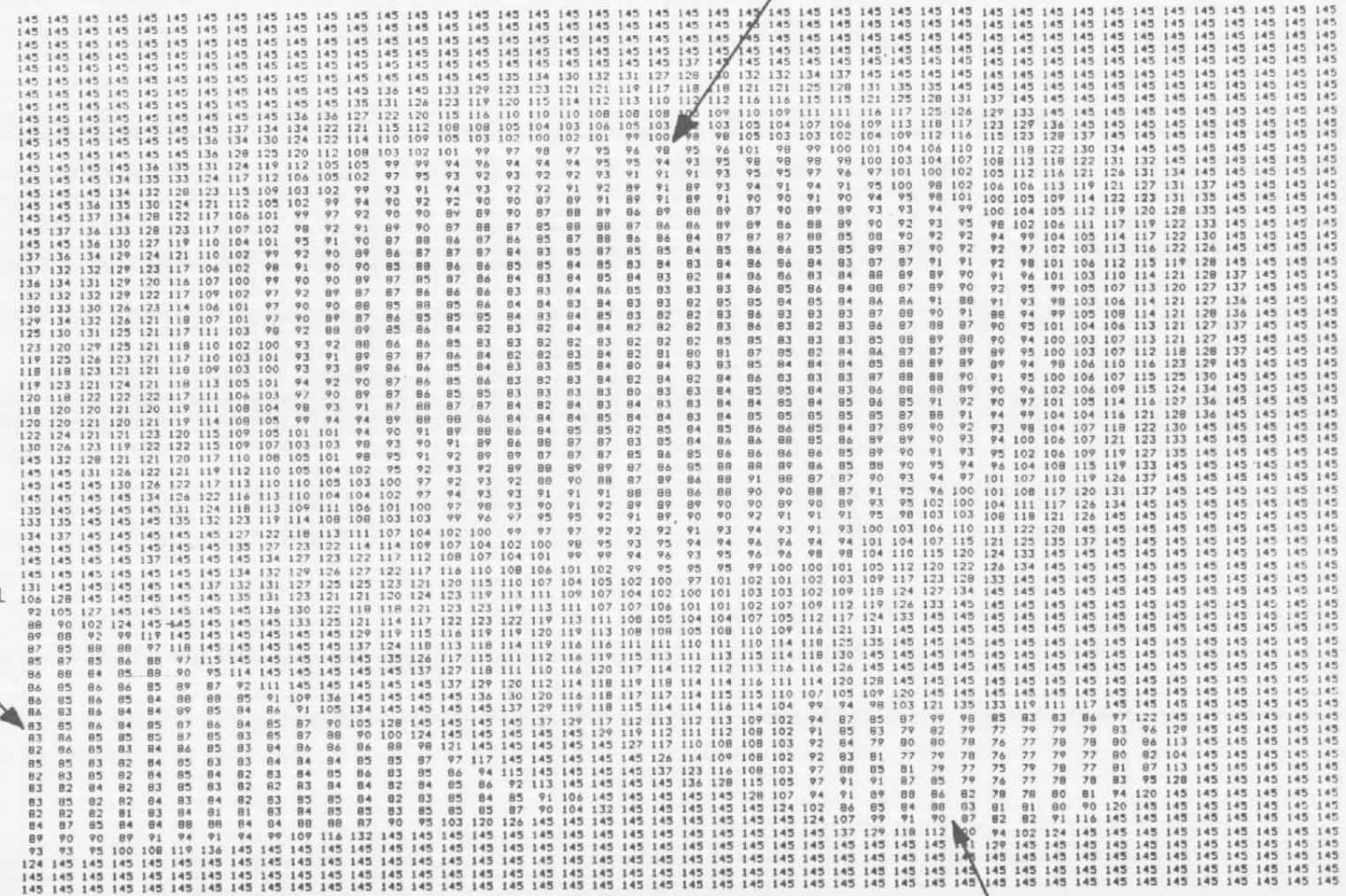


Figure 31. Digital data - pixel grey level array of a vortex.

## REFERENCES

1. O'Hare, J. E., Trolinger, J. D., Farmer, W. M., and Belz, R. A. "Holographic Flow Visualization." UTSI-AIAA Weekend Workshop Proceedings on "Applied Measuring Techniques," February 1969.
2. O'Hare, J. E. "A Holographic Flow Visualization System." SPIE Symposium Proceedings, August 1969.
3. O'Hare, J. E. and Trolinger, J. D. "Holographic Color Schlieren." *Applied Optics*, October 1969, pp. 2047-2050.
4. Trolinger, J. D. and O'Hare, J. E. "Aerodynamic Holography." AEDC-TR-70-44 (AD709764), August 1970.
5. Trolinger, J. D., Belz, R. A., and O'Hare, J. E. "Holography of Nozzles, Jets, and Spraying Systems." *Progress in Astronautics and Aeronautics*, Vol. 34, Instrumentation for Air Breathing Propulsion, 1974.
6. Strike, W. T., O'Hare, J. E., and Templeton, W. L. "Development of Holographic Interferometric Applications in the VKF Supersonic and Hypersonic Wind Tunnels." AEDC-TR-75-1 (ADA007689), April 1975.
7. Trolinger, J. D. "Laser Instrumentation for Flow Field Diagnostics." AGARDograph No. 186, March 1974.
8. Abramson, N. "Sandwich Hologram Interferometry: A New Dimension in Holographic Comparison." *Applied Optics*, Vol. 13, No. 9, September 1974, pp. 2019-2025.
9. "EyeCom Handbook." Spatial Data Systems, First Edition, 1977.
10. Van Houten, P. E. "The Application of Holographic Interferometry to the Determination of Discontinuous Three-Dimensional Density Fields." Naval Postgraduate School, Monterey, CA, Thesis, December 1972.
11. Dungier, R. H. "A Computational Method for Exact, Direct, and Unified Solutions for Axisymmetric Flow Over Blunt Bodies of Arbitrary Shape (PROGRAM BLUNT)." AFWL-TR-70-16, July 1970.
12. Inouye, M., Rakich, J. V., and Lomax, H. "A Description of Numerical Methods and Computer Programs for Two-Dimensional and Axisymmetric Supersonic Flow over Blunt-Nosed and Flared Bodies." NASA TN D-2970, August 1965.